POLITECNICO DI TORINO
Repository ISTITUZIONALE

A Game of Social Forces: Integrating Non-cooperative Game Theory with Social Force Model for a Socially-acceptable Mobile Robot Navigation

Original
A Game of Social Forces: Integrating Non-cooperative Game Theory with Social Force Model for a Socially-acceptable Mobile Robot Navigation / Galati, G., Usai, A., Vignolo, G., Macrì, S., Rizzo, A.. - In: JOURNAL OF INTELLIGENT & ROBOTIC SYSTEMS. - ISSN 1573-0409. - 111:(2025). [10.1007/s10846-025-02318-0]

Availability:
This version is available at: 11583/3003788 since: 2025-10-08T09:18:34Z

Publisher:
Springer

Published
DOI:10.1007/s10846-025-02318-0

Terms of use:

This article is made available under terms and conditions as specified in the corresponding bibliographic description in the repository

Publisher copyright

(Article begins on next page)

26 November 2026

Journal of Intelligent & Robotic Systems (2025) 111:110
https://doi.org/10.1007/s10846-025-02318-0

REGULAR PAPER

A Game of Social Forces: Integrating Non-cooperative Game Theory with Social Force Model for a Socially-acceptable Mobile Robot Navigation

Giada Galati[1] · Andrea Usai[1] · Giacomo Vignolo[1] · Simone Macrì[2] · Alessandro Rizzo[1]

Received: 16 April 2025 / Accepted: 23 September 2025
© The Author(s) 2025

Abstract
Robot integration in daily life demands research on both safety and social acceptance. Current methods focus on safety, but social factors are understudied. Moreover, existing studies lack deep analysis of human perception towards robot movement. Here, we present a novel navigation approach based on the combination of Game Theory and the Social Force Model (GTSFM) to bridge these gaps. We model navigation as a non-cooperative game to consider both pedestrians and robot as rational agents influencing each other's choices. We evaluate the social acceptability of the GTSFM algorithm from both quantitative and qualitative perspectives. In both evaluations, the GTSFM is compared against two state-of-the-art algorithms: the social force model (SFM) and the optimal reciprocal collision avoidance (ORCA). According to the quantitative analysis performed in simulation, the GTSFM outperforms the SFM in all considered performance metrics and ensures higher performance than ORCA considering the smoothness of the trajectories and the proximity to pedestrians. The qualitative measurement is performed through a real-world experiment using a questionnaire administered to a pool of 76 participants. Our qualitative analysis revealed no statistically significant differences in performance between the algorithms tested. This lack of distinction may be due to unaccounted factors. The robot's appearance and the limited velocity of the real robot could have obscured the distinction between the algorithms. These results represent a significant milestone in advancing the integration of robots into social environments also leave important hints for future research.

Keywords Game theory · Social force model · Socially-acceptable motion planning · Interaction awareness · HRI · Socially-aware navigation

1 Introduction

The boundaries between humans and robots are becoming increasingly blurred. Robots are no longer confined to isolated laboratories and industries but are entering shared spaces, navigating alongside humans in museums [1], homes [2], hospitals [3], streets [4], and offices [5], to name a few.

This growing coexistence presents a challenge: to integrate perfectly, robots should navigate collaboratively with humans, prioritizing not only physical safety but also ensuring a high level of *social acceptability* [6].

Although traditional navigation algorithms excel at planning efficient paths and avoiding obstacles [7], they fail to take into account the social acceptability issue. This is primarily due to the oversimplification of human behavior, which often models humans as inanimate dynamic obstacles rather than social entities engaging in complex and strategic interactions [8]. This oversimplification of human behavior can have critical consequences, leading to situations such as the well-documented "freezing robot problem" [9].

This is where socially-aware navigation emerges as a core approach. Socially-aware navigation gives robots the ability to shift from simple obstacle-avoiding entities to socially-aware participants.

Through sensor fusion and accurate human-motion predictions, robots can: (i) perceive the social environment through sensors; (ii) understand and adhere to social norms;

✉ Alessandro Rizzo
alessandro.rizzo@polito.it

[1] Department of Electronics and Telecommunications, Politecnico di Torino, Torino, Italy

[2] Centre for behavioral Sciences and Mental Health, Istituto Superiore di Sanità, Roma, Italy

Published online: 07 October 2025

(iii) make decisions that are not only collision-free but also socially appropriate, considering factors such as cultural norms, and anticipated human behavior; (iv) plan and execute their movements in a way that is smooth, predictable, and respectful of human space and expectations.

Toward improving trust, comfort, and social acceptance, humans should be explicitly considered by robots as intelligent agents who interact and may influence the motion of others [10]. Recent efforts in socially-aware navigation model humans as static entities [11] or as agents driven by very simplistic motion models [12]. Such simplistic assumptions may hardly cope with the complexity of human behavior and interaction, yielding trajectories that are far from predictable, smooth, and in turn acceptable for humans. Models based on learning theory, on the other hand, promise better results [13] provided that a large training data set involving human subjects is available, which is not always the case.

Game theory is a powerful and flexible mathematical paradigm to study strategic interactions between different components of a system (in our scenario, moving pedestrians) [14]. Because of such flexibility, game theory has rapidly increased in popularity over the past decades and has found application in interdisciplinary studies in multi-agent interactions in many fields, including distributed control [15], epidemiology [16], building evacuation [17, 18], human-unmanned vehicle interaction [19], and multiple robot coordination [20–22].

Game theory offers substantial benefits compared to alternative modeling methods, such as reactive strategies [23–25] and learning schemes [26–29]. With respect to the former, game theory is able to perform motion prediction and anticipation of the behavior of other humans, typical of human decision-making in social contexts [30]. Compared to the latter, it overcomes their distinctive lack of explainability, generalization, and the need for large training data sets.

Despite the well-known ability of game theory to model different aspects of human behavior, only a few efforts have attempted to incorporate it into a mobile robot motion. This limited literature could be attributed to the inherent non-negligible computational complexity of game theory.

Nevertheless, future advancements in the computational power of microcontrollers are expected to make it feasible to implement complex algorithms on modestly sized mobile robots, thus opening the way to the exploration of more demanding game-theory-based approaches.

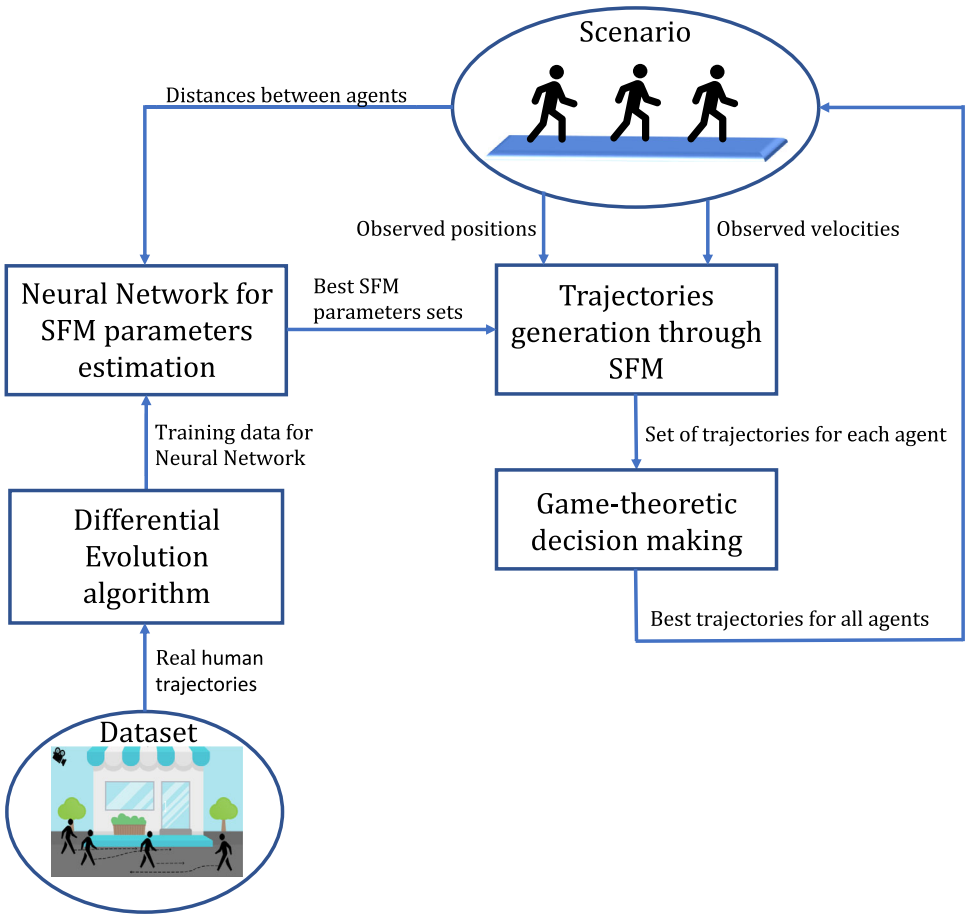


Fig. 1 Conceptual framework of GTSFM with real-time parameters estimation

In this study, we design a robotic trajectory planner for a populated environment that combines game theory [14] and the Social Force Model (SFM) [23], henceforth we refer to it as GTSFM. Game theory is used to choose between four different possible trajectories generated by the SFM. Based on preliminary tests carried out in Gazebo and on the analysis of computational complexity, which grows exponentially as $n_c^{n_p}$ with the number of pedestrians n_p and the number of choices available to each pedestrian n_c, we decided, without loss of generality, to limit the number of choices per player to four. This configuration provided a suitable balance between computational efficiency, the ability to incorporate human anticipation into the algorithm, and sufficient diversity in pedestrian behaviors.

To generate pedestrian trajectories, we computed different sets of SFM parameters through a Differential Evolution algorithm (DE) [31]. The latter relied on real human motion data as the ground truth, guiding the optimization process towards trajectories exhibiting high levels of naturalness and human-likeness. Although the DE algorithm offers powerful parameter estimation capabilities, its high computational demand limits its application in real-time scenarios. This study addresses this limitation by proposing a neural network to mimic the DE algorithm, allowing real-time parameter estimation. The general structure of our GTSFM algorithm is illustrated in Fig. 1.

In this study, we leverage the concept of anthropomorphism, i.e. the innate human inclination to attribute intentions and consciousness to entities that are non-human [32]. This attribution can be leveraged strategically during trajectory design. This approach has been shown to improve the acceptability of robots by humans [33]. Thus, by incorporating aspects of human movement into robotic trajectories, through the tuning of the SFM parameters with real human trajectories, we aim to improve the perceived acceptance of the robot by humans.

Following the formalization of the GTSFM algorithm, a two-fold validation is conducted: (i) a *quantitative* evaluation of GTSFM is performed in simulated scenarios (Fig. 2) to assess its efficiency, smoothness, and perceived comfort. GTSFM is compared against two state-of-the-art algorithms: SFM [23] and Optimal Reciprocal Collision Avoidance (ORCA) [34]; (ii) a *qualitative* evaluation of GTSFM is conducted through a real-world experiment using a real robot, to measure the anthropomorphism of the GTSFM compared to SFM and ORCA (Fig. 3).

Our *quantitative* evaluation demonstrates that GTSFM generates significantly smoother paths than SFM and ORCA, potentially resulting in more natural robot motion. Additionally, GTSFM outperforms the standard SFM model across all performance metrics, indicating improved navigation efficiency and trajectory quality.

While our *qualitative* analysis did not reveal a clear superiority of one algorithm over the others, this could be due to unaccounted factors. The robot's appearance and limited velocity may have constrained the range of tested conditions, obscuring potential differences between the algorithms.

2 Related Works

As outlined in [35], existing socially-aware navigation approaches can be categorized into *model-based* and *learning-based methods*.

Model-based algorithms rely on human-motion mathematical models, like geometric rules or physics equations, to enable the navigation robot process. On the other hand, *learning* algorithms learn from real human motion data, allowing them to better mimic human behavior in navigation.

Many state-of-the-art approaches to socially-aware navigation rely on *model-based* methods, such as the SFM [23]. SFM uses attractive and repulsive forces to simulate human-like movement based on the laws of Newtonian mechanics. Motivated by the potential of the model for broader applicability, subsequent research has extended the capabilities of the SFM by incorporating additional forces [36, 37]. Another notable model-based algorithm is the Velocity Obstacle (VO), introduced by Fiorini and Shiller in 1998 [38]. The VO generates avoidance maneuvers by determining a permissible velocity for the robot outside the collision cone. However, VO does not consider reciprocal mutual avoidance typical of human behavior during navigation. To address this

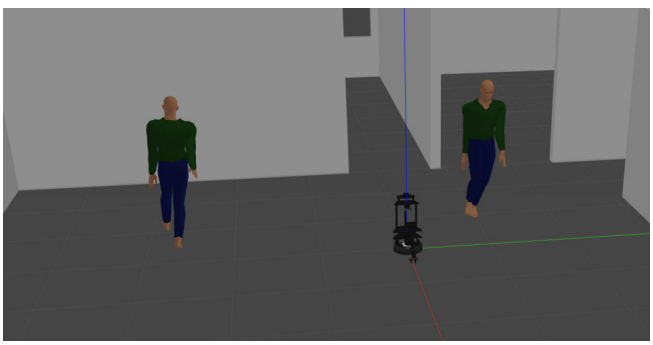


Fig. 2 Simulated scenario for *quantitative* evaluation



Fig. 3 Real-world experiment for *qualitative* evaluation with two humans and the robot

limitation, Berg et al. [39] proposed the Reciprocal Velocity Obstacle (RVO). While RVO improves collision avoidance, it lacks a definitive guarantee for all scenarios (such as when both agents choose the speed inside each other's RVO). To overcome this problem, RVO was further refined in [34] with ORCA.

While the algorithms presented above adopt a reactive approach, focusing on immediate obstacle avoidance, certain model-based methods go beyond this limitation by incorporating predictions of pedestrian behavior within a specified time horizon. An example of such approaches is the game theory method to design motion planning for a mobile robot.

While game theory is adept at modeling human behavior, its application to mobile robot motion remains limited. In this context, Turnwald et al. [30] modelled human navigation as a non-cooperative game. The core contribution of their work lies in real-world experiments on how pedestrians choose trajectories based on achieving a Nash equilibrium. The same author in [10], investigates how the game-theoretic human model can be further adapted for designing a human-like motion planning. Building upon analogous theoretical foundations, Galati et al. [40] propose a game-theoretical social-aware navigation algorithm including group recognition, sequential decision making and human-obstacle interaction.

While the *model-based* approaches have impressive advantages like rapid implementation without a training process with data and generalizability to a more complex environment, they face certain limitations. Firstly, the lack of human-like behavior training with real data might lead to unnatural navigation patterns, potentially causing confusion or discomfort for humans in shared spaces. Secondly, fine-tuning the model's parameters for optimal performance can be a complex and time-consuming task.

On the other hand, the continuous advancements in deep learning technology and the integration of deep neural networks are contributing to the growing popularity of *learning-based* approaches for robotic navigation. The learning-based approaches can be divided into three classes according to their different working principles: (i) supervised learning leverages real-world pedestrian trajectory data to train networks that capture and reproduce the social interactions observed in human navigation [41, 42]; (ii) deep reinforcement learning mimics the way animals and humans learn, adapting their behavior based on rewards. An example of this method is adopted in [13, 43, 44]; (iii) inverse reinforcement learning: offers a solution by learning from expert demonstrations to automatically deduce the reward structure [45–47].

Unlike *model-based* approaches, *learning-based* methods leverage real-world trajectory data to achieve behavior closer to human navigation. However, this advantage comes at the cost of extensive data requirements for training and limited generalizability beyond the specific training scenarios.

Moreover, the limited interpretability of the output of these methods presents a significant challenge, creating difficulties in comprehending the underlying causes of specific behaviors. Consequently, debugging and diagnosing issues become more complex, thereby posing a major drawback compared to *model-based* methods. In addition, limited interpretability of the outputs in some cases may lead to unexpected and potentially dangerous behaviors in human-shared environments. Careful design of recovery and emergency mechanisms is crucial to ensure the robot's movements remain safe and socially acceptable under all circumstances.

3 Our Contributions

This study proposes a novel trajectory planning approach by combining the SFM with the game theory logic (GTSFM). This combined approach offers significant advantages over existing methods within the model-based and learning-based categories.

With respect to the former, our model extends the current state of the art in many directions. First, our model keeps the computational efficiency of the SFM, while using it to estimate multiple trajectories over a fixed-time horizon for each pedestrian. Second, we incorporate game theory into our approach to determine the optimal trajectory for each individual, taking into account the mutual influences between humans. Third, while similar approaches have been investigated in different contexts, such as in a road-shared space with pedestrians and cars [48], the integration of the SFM and game theory for socially-aware navigation appears to be novel. Fourth, unlike prior works that focus just on binary interactions [49, 50], in our model, each player interacts by playing a game with all other players present in the scene. Furthermore, in contrast to [10], in our model, the decision-making process is calculated at every time step rather than just once, mimicking the sequential nature of human decision-making processes. Finally, our approach can generate human-like trajectories by using a Differential Evolution algorithm, which tries to estimate the best SFM's parameters that approximate real human trajectories as closely as possible.

On the other hand, our proposed approach offers several advantages over learning-based methods. First, it does not require training on a specific scenario. This makes it more generalizable to unforeseen situations, which is crucial for real-world applications. Second, our model provides more interpretable results. This is because it is based on a physics-based model of the human motion (SFM), rather than a black-box learning model. This interpretability is essential for understanding the reasons behind the robot's decisions and for limiting potentially unsafe behaviors.

Since the GTSFM algorithm is built on the SFM, the GTSFM inherits both its strengths and limitations. SFM excels at describing the dynamics of pedestrian movement, but its performance is highly sensitive to the values of its parameters. Slight changes in these parameters can significantly affect the model output, as illustrated in Fig. 4. In addition, the SFM parameters may vary in different navigation scenarios, requiring time-consuming calibration processes.

Moreover, due to calibration challenges, the model often requires a single set of parameters for all agents, which can compromise its descriptive accuracy, as human navigation exhibits significant heterogeneity.

Thus, to address the two problems presented above, we use a DE algorithm to estimate the SFM parameters that best approximate real human trajectories.

The rest of the paper is organized as follows. In Section 4, we give an overall description of our GTSFM approach, followed by a detailed overview of the main building blocks. In Section 5, we illustrate the experiment setup and the metrics used to evaluate the algorithms quantitatively and qualitatively. In Section 6 we present the overall results of the experiment. In Section 7, we discuss the results and outline future research.

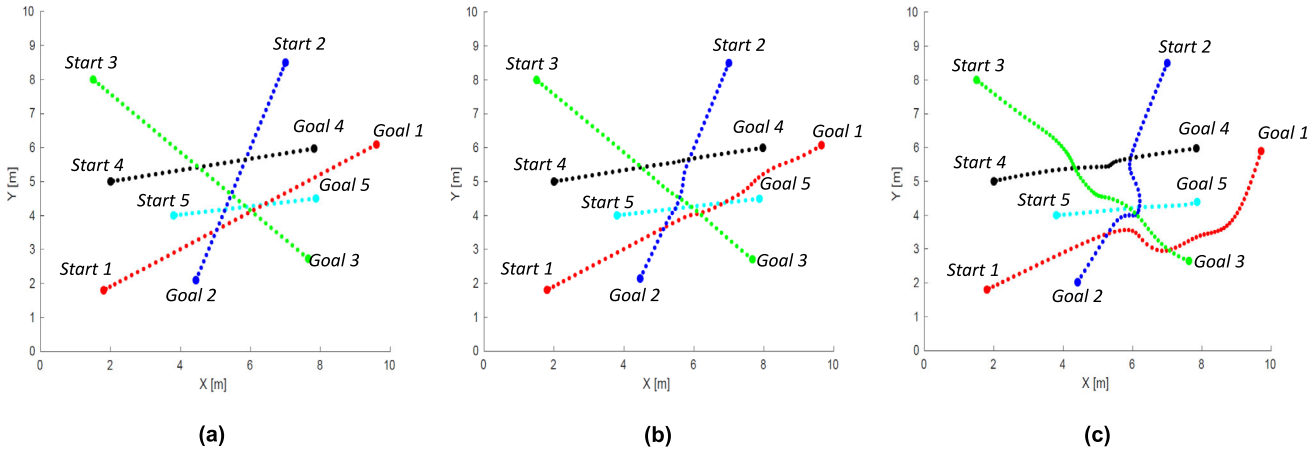


Fig. 4 Simulations with 5 agents controlled by SFM with different sets of parameters: (a) $A_i = 0.2$, $B_i = 0.1$, $r_i = r_j = 0.1$; (b) $A_i = 0.45$, $B_i = 0.3$, $r_i = r_j = 0.4$; (c) $A_i = 1$, $B_i = 0.7$, $r_i = r_j = 0.7$. For illustrative purposes, we introduced variability by adjusting only the pedestrian interaction parameters while assuming that all pedestrians share identical values for the desired speed (v_i^d), relaxation time (α_i), and anisotropic strength (λ)

4 Methodology

4.1 Overview of GTSFM with Real-time Parameters Estimation

In this study, a Game Theory and the Social Force Model (GTSFM) algorithm with real-time parameter estimation is adopted.

Here, we posit that the players of the game are both the robot and humans, as the latter are extensively described by the SFM in the literature [23]. Therefore, from this point onwards, we will use the term "agent" interchangeably to refer to both humans and the robot.

In Fig. 1, the general structure of the algorithm is presented. Specifically, we devise a game whose action set is a finite set of possible trajectories for each agent, generated using the well-established and computationally efficient SFM over a fixed-time horizon. Then, each agent selects its action toward minimizing a cost function that takes into account its willingness to reach its goal, the regularity of its trajectory, and its willingness to avoid interactions with other individuals within its personal space.

To find the best SFM sets of parameters approximating human behavior and generate different trajectories for each agent, a DE algorithm [31] is incorporated in the GTSFM framework, as shown in Fig. 1.

However, the excessive time needed to perform the parameter estimation makes the DE algorithm inadequate for real-time applications. Thus, to overcome this issue, the DE algorithm is mimicked by a neural network. The latter is trained with supervised data, leveraging a labelled dataset created by the DE algorithm. The labelled dataset associates specific features of the scenario, such as the distance between agents, with the optimal parameters for the SFM.

To compute the optimal parameters for the training dataset, the DE algorithm computes the best sets of parameters for the SFM that approximate real human trajectories of a public dataset (Thör [51]). The proposed logic is used to design a robotic trajectory planner in a populated environment.

In the following Subsections a detailed explanation of the constituent elements of the GTSFM is presented. Section 4.2 delineates the underlying principles of the *social force model*. Section 4.3 provides a structured framework for the usage of *game theory* in modelling the navigation process. Section 4.4 furnishes insights into the dataset employed by the DE algorithm. Section 4.5 explains how the DE algorithm is used to estimate the SFM parameters. Additionally, Section 4.6 details an overview of the *neural network* needed for real-time SFM parameter generation. Each of these components is elucidated individually and comprehensively.

4.2 SFM

The SFM was introduced by D. Helbing and P. Molnar in [23] to reproduce the motion of humans in an environment. Over the years, numerous scholars have suggested various enhancements to refine and improve the Helbing model [52–54]. In this study, we are inspired by the works of Helbing [23] and Ferrer [53].

The SFM considers a set $\mathcal{N} = \{1, \dots, n\}$ of $n \in \mathbb{N}$ agents, who move in a continuous planar space $X \in \mathbb{R}^2$. Each agent $i \in \mathcal{N}$ is characterized by a goal $\mathbf{p}_i^{\text{goal}} \in \mathbb{R}^2$, that is the final position that the agent wants to reach, and two time-varying vectors that determine its current state: its position $\mathbf{p}_i(t) \in \mathbb{R}^2$ and its velocity $\mathbf{v}_i(t) \in \mathbb{R}^2$. Position and velocity evolve in continuous time, $t \in \mathbb{R}_{\geq 0}$. The motion of each agent is governed by a set of forces. In particular, the model includes an attractive force $\mathbf{F}_i^{\text{goal}}$, which drives the agents toward their goals, a set of interaction repulsive forces of the form $\mathbf{F}_{ij}^{\text{int}}$, which makes agent i to avoid colliding with agent j, and a repulsive force $\mathbf{F}_i^{\text{obs}}$ related to the proximity of the agent to a static obstacle or wall.

The motion of the generic i-th agent is obtained by representing the agent as a particle complying with the laws of Newtonian mechanics. The equations of motion of agent i are given by the following system of ordinary differential equations discretized with a time step Δ_t:

$$\begin{aligned} \mathbf{v}_i(t+\Delta_t) &= \mathbf{v}_i(t) + \Delta_t \left[\mathbf{F}_i^{\text{goal}}(t) + \sum_{j \in \mathcal{N} \setminus \{i\}} \mathbf{F}_{ij}^{\text{int}}(t) + \mathbf{F}_i^{\text{obs}}(t) \right] \\ \mathbf{p}_i(t+\Delta_t) &= \mathbf{p}_i(t) + \Delta_t \mathbf{v}_i(t), \end{aligned} \tag{1}$$

where in the first equation we assume, without any loss in generality, that forces are re-scaled so that all agents have unitary mass.

In the following, we detail the three types of forces present in Eq. 1:

Attractive force: Agent i is attracted to its goal $\mathbf{p}_i^{\text{goal}}$ by means of the driving force $\mathbf{F}_i^{\text{goal}}(t)$. Specifically, fixed a scalar parameter $v_i^d > 0$, which is the desired velocity of the agent toward its goal, we define

$$\mathbf{F}_i^{\text{goal}}(t) = \frac{v_i^d \widehat{\mathbf{e}}_i(t) - \mathbf{v}_i(t)}{\alpha_i}, \tag{2}$$

where $\widehat{\mathbf{e}}_i(t) = \frac{\mathbf{p}_i^{\text{goal}} - \mathbf{p}_i(t)}{\left\| \mathbf{p}_i^{\text{goal}} - \mathbf{p}_i(t) \right\|}$ is the desired direction (i.e., the normalized vector that points toward the agent's goal) and $\alpha_i \in \mathbb{R}_{>0}$ is a parameter that captures the relaxation time. The latter regulates the rate of change of the agent –

a smaller values mimic a stronger tendency to decisively move toward the goal.

Interaction forces: The interaction with other agents influences the motion of agent i. Agents tend to feel uncomfortable when unknown agents get close to their personal space and consequently try to avoid this situation [55]. In the SFM, the interaction of agent i with agent j is modeled with a repulsive force F_{ij}^{int} (defined for all $j \in \mathcal{N} \setminus \{i\}$). We denote by $r_i, r_j > 0$ the radii of the personal spaces of agents i and j, respectively (i.e., the region around humans in which others cannot intrude without causing discomfort [56]), and by $d_{ij}(t) := ||\mathbf{p}_i(t) - \mathbf{p}_j(t)||$ the distance between the two agents. Then, the interaction force is defined as

$$\mathbf{F}_{ij}^{\text{int}}(t) = A_i \exp\left\{\frac{r_i + r_j - d_{ij}(t)}{B_i}\right\} F_{i,j}^{fov}(t)\widehat{\mathbf{n}_{ij}}(t), \quad (3)$$

where the constant parameters $A_i, B_i \in \mathbb{R}_{>0}$ regulate the strength and range of the interaction force for agent i, respectively. $F_{i,j}^{fov}(t) \in [0, 1]$ is a (time-varying) scaling factor, associated with the agent's field of view, detailed in the following, and $\widehat{\mathbf{n}_{ij}}(t) = \frac{\mathbf{p}_i(t) - \mathbf{p}_j(t)}{\|\mathbf{p}_i(t) - \mathbf{p}_j(t)\|}$ is the direction between the two agents.

Since agents have a limited field of view when walking and are affected mainly by the objects within their field of view, the repulsive force is scaled by an anisotropic factor $F_{i,j}^{fov}(t) \in [0, 1]$ depending on the bearing $\gamma_{ij}(t)$ of agent j, measured from agent i[1].

Such a factor is defined as

$$F_{i,j}^{fov}(t) = \lambda + (1 - \lambda)\frac{1 + \cos(\gamma_{ij}(t))}{2}, \quad (4)$$

where $\lambda \in [0, 1]$ is the strength of the anisotropic behavior: the closer λ is to one, the smaller the impact of a limited field of view.

Repulsive forces from obstacles/walls: During navigation, an agent naturally maintains a specific distance from the edges of buildings, walls, and obstacles. The discomfort increases as the individual approaches a border, as greater attention is required to avert the risk of injury, such as accidental contact with a wall. Consequently, a border of a generic obstacle elicits a repulsive effect, which is characterized by the following expression:

$$\mathbf{F}_i^{obs}(t) = A_{obs} \exp\left\{\frac{r_i + r_o - d_{i,obs}(t)}{B_{obs}}\right\} F_{i,obs}^{fov}(t)\widehat{\mathbf{n}}_{i,obs}(t), \quad (5)$$

where the constant parameters $A_{obs}, B_{obs} \in \mathbb{R}_{>0}$ regulate the strength and range of the interaction force for agent i, respectively. $r_i, r_o > 0$ are the radius of the personal spaces of agents i and a value to model a safety distance from the nearest point of the nearest obstacle, respectively. $d_{i,obs}(t) := ||\mathbf{p}_i(t) - \mathbf{p}_o(t)||$ is the distance between the agent i and the obstacle. As discussed for the repulsive force between agents (Eq. 3), also the repulsive force for obstacle is scaled by a corresponding anisotropic factor $F_{i,obs}^{fov}(t)$ defined as follows:

$$F_{i,obs}^{fov}(t) = \lambda + (1 - \lambda)\frac{1 + \cos\gamma_{i,obs}(t)}{2} \quad (6)$$

where $\lambda \in [0, 1]$ is the strength of the anisotropic behavior: the closer λ is to one, the smaller is the impact of a limited field of view, and $\gamma_{i,obs}(t)$ is the bearing angle of the considered obstacle measured from agent i. Moreover, in the definition of the Eq. 5, there is $\widehat{\mathbf{n}}_{i,obs}(t)$, i.e. direction between the agent i and the nearest point of the nearest obstacle defined as $\widehat{\mathbf{n}}_{i,obs}(t) = \frac{\mathbf{p}_i(t) - \mathbf{p}_o(t)}{\|\mathbf{p}_i(t) - \mathbf{p}_o(t)\|}$.

All the parameters of the SFM are summarized in Table 1.

4.3 Game-theoretic Formalization

Here, we present a game-theoretic methodology which is a non-cooperative, static, perfect information, and finite game with a finite number of agents. In our game, each agent aims to achieve its own goal *individually*.

In the proposed GTSFM, the n agents $\mathcal{N} = \{1, \ldots, n\}$ move according to the SFM and use a game-theoretic mechanism to find the best set of parameters to generate the best trajectory to reach the goal and avoid other agents.

Specifically, at each time step t, agent i has a finite set $\mathcal{S}_i$ of possible actions. These latter represent possible sets of SFM parameters. To each action $a \in \mathcal{S}_i$, we associate the corresponding trajectory for agent i, denoted as τ_i^a. We leverage a cost function $J(\tau_i^a)$ to associate a cost to each trajectory $\tau_i^a \in \mathcal{S}_i$. The objective of each agent is to minimize its respective cost function.

Here, similar to [30], we posit that the optimal behavior for humans is the convergence to a Nash equilibrium, a situation where no agent has an incentive to unilaterally change their action without the others changing theirs.

In the following, we provide the details on the cost function defined for the GTSFM, we illustrate the method used to compute the Nash equilibria of the game, and we finally summarize our motion algorithm.

Cost Function We assume that agents have perfect information, that is, they have information about the current actions of other agents. This assumption is realistic, considering the

[1] More specifically, the bearing $\gamma_{ij}(t)$ is the angle between the direction of motion of agent i and the segment joining the positions of agent i and agent j.

Table 1 Model variables and parameters

Symbol	Meaning
n	number of agents
$X \in \mathbb{R}^2$	planar space
$\mathbf{p}_i(t) \in \mathbb{R}^2$	position of agent i at time t
$\mathbf{v}_i(t) \in \mathbb{R}^2$	velocity of agent i at time t
$\mathbf{p}_i^{\text{goal}} \in \mathbb{R}^2$	position of the goal of agent i
$\mathbf{F}_i^{\text{goal}} \in \mathbb{R}^2$	attractive force for agent i at time t
$\mathbf{F}_i^{obs}(t) \in \mathbb{R}^2$	repulsive force of the closest obstacle on agent i at time t
$\mathbf{F}_{ij}^{\text{int}}(t) \in \mathbb{R}^2$	interaction force of agent j on i at time t
$r_i \in \mathbb{R}_{>0}$	radius of the personal space of agent i
$r_j \in \mathbb{R}_{>0}$	radius of the personal space of agent j
$v_i^d \in \mathbb{R}_{>0}$	desired velocity (in modulus) of agent i
$\alpha_i \in \mathbb{R}_{>0}$	relaxation time of agent i
$A_i \in \mathbb{R}_{>0}$	strength of interaction force for agent i
$A_{obs} \in \mathbb{R}_{>0}$	strength of repulsive force from obstacle i
$B_i \in \mathbb{R}_{>0}$	range of interaction force for agent i
$B_{obs} \in \mathbb{R}_{>0}$	range of repulsive force from obstacle
$\gamma_{ij}(t) \in \mathbb{R}$	bearing of agent j measured by agent i
$F_{i,j}^{fov} \in [0, 1]$	anisotropic factor in agent interaction
$F_{i,obs}^{fov} \in [0, 1]$	anisotropic factor for agent-object interaction
$\gamma_{i,obs}(t) \in \mathbb{R}$	bearing of the nearest obstacle measured by agent i
$\lambda \in [0, 1]$	strength of anisotropic behavior

inherent human characteristic of interpreting others' behavior and predicting their motion [30].

Using the SFM and the perfect information assumption, each agent can compute the trajectory associated with each parameters set. In particular, each trajectory is computed by using Eq. 1 over a fixed-time horizon ($T_{\text{prev}}\Delta_t$), where T_{prev} is the number of time-steps and Δ_t is the duration of each time-step. To enhance clarity and without sacrificing generalizability, here and henceforth, we assume a unitary discrete-time step, i.e. Δ_t=1.

Finally, to evaluate the cost of each generated trajectory (τ_i^a) for the i-th agent, we define the cost function $J(\tau_i^a)$ as the sum of three contributions:

$$J(\tau_i^a) = \Phi_{\text{goal}}(\tau_i^a) + \Phi_{\text{smooth}}(\tau_i^a) + \Phi_{\text{int}}(\tau_i^a). \tag{7}$$

Such a cost function is built on the cost function proposed in [40] by part of the authors, enriched with a term that accounts for the willingness to engage in social interaction. Details on the three summands are given in what follows.

The first term is defined as

$$\Phi_{\text{goal}}(\tau_i^a) = \sum_{k=1}^{T_{\text{prev}}} \|\mathbf{p}_i(t+k) - \mathbf{p}_i^{\text{goal}}\|, \tag{8}$$

and accounts for the path length for agent i. Hence, minimizing such a term captures the goal-oriented attitude of the agent.

The second term is defined as

$$\Phi_{\text{smooth}}(\tau_i^a) = \sum_{k=1}^{T_{\text{prev}}} |\theta_i(t+k) - \theta_i(t+(k-1))|, \tag{9}$$

where $\theta_i(t+k)$, $\theta_i(t+(k-1))$ are the orientation (angle) of the agent at time-step $(t+k)$ and $(t+(k-1))$, respectively. Such a term penalizes excessive rotations, thus promoting smooth trajectories. In fact, during navigation, humans tend to avoid too many changes of orientation to minimize their energy consumption [57].

The third term is defined as

$$\Phi_{\text{int}}(\tau_i^a) = \sum_{j \in \mathcal{N}\setminus\{i\}} \sum_{k=1}^{T_{\text{prev}}} \frac{\rho}{\|\mathbf{p}_i(t+k) - \mathbf{p}_j(t+k)\|}, \tag{10}$$

where $\rho \in \mathbb{R}_{\geq 0}$ is a (constant) weighting factor, and the denominator in Eq. (10) is the distance between the agent position $\mathbf{p}_i(t+k)$ and the other agents $\mathbf{p}_j(t+k)$ at time-step $(t+k)$. Hence, by minimizing this term, agents tend to maintain a safe distance from others. The weighting factor ρ determines the relative weight of this term with respect to

the other two in the cost function and, ultimately, the radius of the agents' personal space.

Numerical Computation of Nash Equilibria Following [30], we assume that agents during navigation tend to converge to a Nash equilibrium. This refers to a situation where no agent has an incentive to unilaterally change its action without the others changing theirs.

However, the existence and uniqueness of a Nash equilibrium cannot be guaranteed in our setup, and its analytical characterization is unattainable. Therefore, we use numerical methods to compute an approximate Nash equilibrium, specifically through the *sequential best response* approach [58]. To describe the concept of sequential best response, we propose the following example that involves two agents.

Example 1 Consider two agents, termed i and j. Agent i observes the navigation of agent j at time t and chooses the best trajectory to reach its own goal, given the latest observed motion of agent j. Subsequently, in each iteration, a check action is taken to confirm whether both agents' strategies remain unchanged from the previous iteration; in such a case, the game has reached a Nash equilibrium. Otherwise, agent j computes its optimal strategy based on the latest strategy of agent i. This iterative process continues until the equilibrium is met. The presented logic can be extended to n agents.

The game-theoretical trajectory planning is implemented following the logic shown in Algorithm 1. During its main loop, Algorithm 1 invokes the game-theoretical strategy selection outlined above, which logic is described in Algorithm 2.

Algorithm 1 Main algorithm of GTSFM trajectory planning.

$\mathbf{p}_{robot} \leftarrow$ InitializeRobotPosition
$\boldsymbol{\tau} \leftarrow$ FirstEstimation [straight paths for all agents]
while $\mathbf{p}_{robot} \neq \mathbf{p}_{goal}$ **do**
  $k \leftarrow 1$ [iteration index]
  $\boldsymbol{\tau}^k \leftarrow \boldsymbol{\tau}$
  while $\boldsymbol{\tau}^k \neq \boldsymbol{\tau}^{(k-1)}$ **do**
    $k \leftarrow k + 1$
    foreach *agent i (robot included)* $\in N$ **do**
      $(\tau_i^*)^k \leftarrow$ StrategySelection $(i, \boldsymbol{\tau})$
  $\mathbf{p}_{robot} \leftarrow$ UpdateRobotPosition

4.4 Dataset for DE Algorithm

To determine the optimal sets of parameters for SFM, the DE algorithm requires a dataset comprising real human trajectories as input.

Algorithm 2 Computation of the actions with the SFM and strategy selection for an agent.

StrategySelection $(i, \boldsymbol{\tau})$
  foreach *action a* **do**
    while $t < T_{prev}$ **do**
      $\frac{\mathrm{d}v_i}{\mathrm{d}t} = \mathbf{F}_i^{\mathrm{goal}}(t) + \sum_{j \in \mathcal{N}\setminus\{i\}} \mathbf{F}_{ij}^{\mathrm{int}}(a,t) + \mathbf{F}_i^{\mathrm{obs}}(t)$
      $v_i(t) = v_i(t - \Delta t) + \frac{\mathrm{d}v_i}{\mathrm{d}t}$
      $\mathbf{p}_i(t) = \mathbf{p}_i(t - \Delta t) + v_i(t)\Delta t$
      $t = t + \Delta t$
    $(J(\tau_i^a)) \leftarrow$ CostComputation(τ_i^a)
  $(\tau_i^*)^k \leftarrow$ MinimizationCost$(J(\boldsymbol{\tau_i}))$
  return $(\tau_i^*)^k$

In this work, the Thör [51] dataset is used, since it is an open-source dataset of human motion trajectories in a controlled indoor environment. In the Thör dataset, three types of scenarios are recorded:

1. *One obstacle:* pedestrians move in the environment without robots, with only a static obstacle positioned at the center of the laboratory room;
2. *Moving robot:* pedestrians and robot move in the same laboratory room, with a static obstacle strategically positioned at the center of the room. The robot used in the experiment is programmed to exhibit *socially unaware behavior*, adhering to a predetermined path around the room and maintaining a constant speed and trajectory without adjustments for the presence of surrounding humans;
3. *Three obstacles:* similar to the first scenario, pedestrians move in the laboratory room in the absence of any robots. However, in this case, three static obstacles are present within the room.

To compute the best sets of parameters, we exclude the use of the second scenario because the robot moves in an unaware manner. This situation could create some biases in the movement of the agents, resulting in a computation of biased parameters, and we aim to avoid this. Moreover, we also exclude the third case because the recorded trajectories are highly dependent on the placement of obstacles in the room. Thus, to compute the best sets of parameters for the SFM, we used only the first scenario, which seems to be the most generalizable scenario among the three.

4.5 DE Used to Estimate Realistic SFM Parameters

This study employs the DE due to its advantageous features over the state-of-the-art algorithms, such as the Evolutionary algorithms (EA) [31]. Unlike many EAs, such as the Genetic Algorithm, DE eliminates the need for encoding

real-valued parameters into bit strings, leading to reduced computational complexity and implementation effort. Additionally, its implementation requires minimal lines of code, making it accessible to researchers across diverse fields. Furthermore, DE's performance depends on tuning just a few well-studied control parameters (population size, mutation factor, and crossover rate), facilitating efficient control parameter tuning.

Due to these characteristics, the DE has become one of the most popular optimization algorithms used in research [31]. DE's versatility has made it a popular optimization algorithm in various fields, including aircraft control [59], robot localization [60], and trajectory planning [61].

Taking inspiration from the work of Johansson et al. [62], our implemented DE algorithm replaces each pedestrian in the Thör dataset (one at a time) with a simulated robot. Such simulated robot moves using the SFM. Specifically, it will start from the same position as the real substituted pedestrian and move for successive T_{prev} time steps Δ_t. This makes it possible to compare the positions reached by the simulated robot driven by SFM with the actual positions reached by the real substituted pedestrian.

This comparison will be executed during the selection phase using the following fitness function:

$$f(\mathcal{X}) = \frac{\sum_{k=t}^{(t+\Delta_t T_{prev})} \|\mathbf{p}_{robot}(k) - \mathbf{p}_{pedToSub}(k)\|}{N} \tag{11}$$

where N represents the total number of points in the trajectory generated by SFM. Such fitness function takes in consideration the average value of the cumulative error between the approximated position $\mathbf{p}_{robot}$ and the real pedestrian position $\mathbf{p}_{pedToSub}$ over T_{prev} time step of the considered trajectory.

For completeness, in Table 2 we summarize the final value of the control parameters of the Differential Evolution algorithm applied in this work. For more details regarding the DE algorithm, please refer to [31].

Algorithm Description The proposed algorithm is used to estimate the $D = 7$ main parameters of the Social Force Model specifically A_i, B_i, r_i, R_0, λ, v_i, α_i of the i-th pedestrian.

Table 2 Control parameters of the implemented DE algorithm

Symbol	Value	Meaning
NP	42	Number of chromosomes in the population
NG	90	Number of generations
F	0.5	Mutation factor
Cr	0.6	Crossover rate

The main steps to obtain the SFM parameters with DE, applied to the Thör dataset are summarized in Algorithm 3.

The inputs of the Algorithm 3 are: the duration of each time-step Δ_t, the number of simulated time-steps T_{prev}, and the Thör dataset. The latter contains different trajectories for each pedestrian. Every point along each trajectory is identified by a tuple *(x, y, t)*, which contains the coordinates in the 2-D plane and the corresponding time t. For each pedestrian pedReal belonging to the Thör dataset, the algorithm saves all trajectories in PedTrajectoriesInfo using the function getTrajectoriesInfo (line 3). In this way, all the start, goal positions, and the instant of reaching the goal (T^{tr}_{goal}) for each trajectory (tr) are known.

Then, for each trajectory, the DE is applied (line 4) until the time t achieves the T^{tr}_{goal} (line 5). Moreover, at each time t the DE is used to simulate over a fixed time horizon $T_{prev}\Delta_t$. Thus, it is necessary to ensure that the simulated trajectory does not extend beyond the real one (line 6). If the simulated trajectory goes beyond the real one, then the algorithm proceeds to the next trajectory (line 7). Otherwise, the best parameters of the SFM that approximate the real trajectory over the time interval $[t; (t + \Delta_t T_{prev})]$ are estimated (line 8).

Then, the initial position of the robot is set to the position of the real pedestrian (line 9). In line 10, the distance between the robot and the closest obstacle is computed. Then, from line 11 to 13, the distances between the robot and the three nearest pedestrians are computed. The estimation of the best four parameter sets is accomplished using the function BestEstPar, as indicated in line 15. The inputs of this function are: all the control parameters of the DE algorithm (NP, F, Cr, NG), the boundaries of the intervals for all D parameters $(\boldsymbol{X}_{min}, \boldsymbol{X}_{max})$, and the information regarding the simulation (Δ_t, T_{prev}). Ultimately, the four distances are associated with the four sets of estimated parameters that most accurately approximate that section of the trajectory (line 16). This part is crucial for generating a sufficiently large labelled dataset that can be used as a training dataset for the neural network. At the end of the algorithm, the time of the simulation is updated (line 17).

In Fig. 5, some results of the DE algorithm applied to the Thör dataset are shown. In particular, in green is shown the real human trajectory and in black the trajectory generated by the SFM with the parameter estimated by the DE algorithm.

4.6 Neural Network for Real-time Parameters Estimation

The training and testing phase of the Neural Network (NN), and the use of the NN in the GTSFM algorithm are summarized in Fig. 6.

In particular, for the creation of the NN, a training-labelled dataset obtained from the DE algorithm is used. Then, a

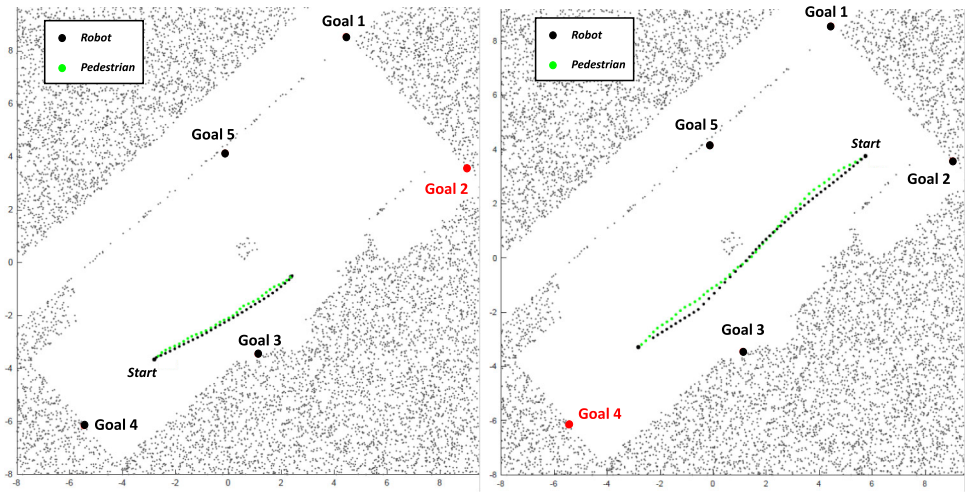


Fig. 5 Comparison between the real human trajectory (in green) and the robot trajectory generated by the SFM with the parameters obtained through the DE (in black)

Algorithm 3 Main algorithm of SFM parameters estimation with DE in Thör dataset.

Input: Δ_t, T_{prev}, ThorDataset
foreach *pedReal* $\in$ *ThorDataset* **do**
  PedTrajectoriesInfo $\leftarrow$ GetTragectoriesInfo(pedReal)
  foreach *tr* $\in$ *PedTrajectoriesInfo* **do**
    while $t < T^{tr}_{goal}$ **do**
      if $(t + T_{prev}\Delta_t) > T^{tr}_{goal}$ **then**
        break
      else
        $\mathbf{p}_{robot}(t) = \mathbf{p}_{pedReal}(t)$
        $d_{robot,obs}(t) = \|\mathbf{p}_{robot}(t) - \mathbf{p}_{obs}\|$
        $d_{robot,ped_1}(t) = \|\mathbf{p}_{robot}(t) - \mathbf{p}_{ped_1}(t)\|$
        $d_{robot,ped_2}(t) = \|\mathbf{p}_{robot}(t) - \mathbf{p}_{ped_2}(t)\|$
        $d_{robot,ped_3}(t) = \|\mathbf{p}_{robot}(t) - \mathbf{p}_{ped_3}(t)\|$
        $\mathbf{d}_{3closestPed}(t) =$
        $[d_{robot,ped_1}(t), d_{robot,ped_2}(t), d_{robot,ped_3}(t)]$
        bestSets $\leftarrow$
        BestEstPar($NP, F, Cr, NG, \boldsymbol{X}_{min}, \boldsymbol{X}_{max}$,
        Δ_t, T_{prev})
        paramDataset $\leftarrow$
        $[d_{robot,obs}(t), \mathbf{d}_{3closestPed}(t)$, bestSets]
        $t \leftarrow t + \Delta_t$

testing phase is performed, using another dataset obtained from the DE algorithm (Fig. 6a). Once the model has been trained and tested, it is ready to be used in the GTSFM algorithm (Fig. 6b). Indeed, the GTSFM algorithm uses the NN to receive different sets of parameters to generate, through the SFM, the set of trajectories for each agent. Then, the best trajectory for each agent is chosen through the game theory logic.

In this study, the NN is trained and tested using TensorFlow [63], an open-source machine learning framework developed by Google Brain. Then, the final NN is integrated into ROS to ensure the implementation of the navigation algorithm into a mobile robot.

In Fig. 6b, the *inputs*, the *outputs* and the *inner structure* of the NN are highlighted. Starting from the description of the *inputs*, the NN has four input parameters: the distance between the considered agent i and the nearest obstacle, and the distances between the same agent i and the three nearest pedestrians. As a result of this setup, the input layer comprises four neurons.

The *outputs* are a total of 28 parameters, namely 7 parameters for each set, which in this case are 4. As a result of this setup, the output layer comprises 28 neurons. In Fig. 6b, for the purpose of illustration, 4 neurons are represented as outputs of the NN, indicating the 4 sets.

Regarding the *inner structure*, the NN includes three hidden layers containing 200 neurons each. These neurons employ the ReLU (Rectified Linear Unit) function as activation function, to elaborate the combination of inputs from the preceding layer.

To obtain the final NN, the training and testing phases are executed. In both phases, the same metric is used to evaluate

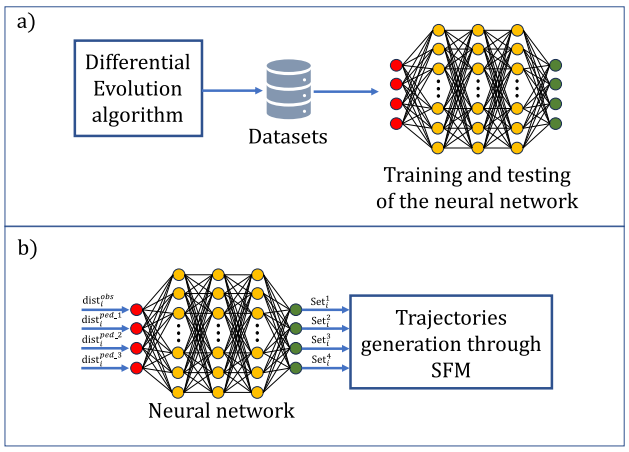


Fig. 6 a) Training and testing of the neural network; b) Neural network in the GTSFM algorithm

performances, i.e. Mean Absolute Error (MAE). In this study, the training phase is executed leveraging the *Adam* optimizer, an optimization algorithm that employs a stochastic gradient descent method. In this phase, a dataset of 420 labelled data is used. In total, the NN is trained for 100 epochs, obtaining a final MAE of 0.2665. In the testing phase, a testing dataset of 100 labelled data is used, obtaining a final MAE of 0.2676.

5 Experiments Design

The experimental phase aims to test the performance of the GTSFM algorithm to evaluate social acceptability from both a *quantitative* and *qualitative* point of view.

While ensuring the social acceptability of algorithms remains challenging due to the inherent subjectivity and context-dependence of the concept, Kruse et al. [6] propose a study that identifies three key approaches to enhancing robot acceptance: human comfort, naturalness, and sociability.

In this study, to measure *quantitatively* the acceptance, we focused mainly on the first two concepts: human comfort and naturalness. The former is ensured through the respect of human personal space. The last is quantitatively evaluated by analyzing the *smoothness* of planned trajectories through performance metrics of the state of the art.

While sociability is an important aspect of human-robot interaction, we have chosen not to focus on this area in our current algorithm development for the *quantitative* phase. This is because sociability can vary greatly depending on the culture and specific situation the robot encounters, and we aim to develop a generalizable algorithm that does not conform to specific social cultures.

The *quantitative* analysis has been conducted through a simulative campaign. The performances of the algorithms have been evaluated using 4 different state-of-the-art metrics: Path Length Ratio (PLR), Average Speed (AS), Closest Pedestrian Distance (CPD) and Path Regularity (PR).

To measure *qualitatively* the acceptability of the GTSFM trajectories we measured the anthropomorphism through the HRIES scale [64], which includes measures regarding *comfort*, *naturalness* and *sociability*.

The *qualitative* analysis has been conducted in a real-world environment with a real mobile robot (Locobot WX-250s) and 2 participants for each experiment. The qualitative assessment of the performance of the algorithms under test has been carried out using a state-of-the-art questionnaire (HRIES) administered to each participant at the end of each experiment.

For an accurate evaluation, in both analyses, the GTSFM has been compared with two other widely used state-of-the-art approaches: the SFM and ORCA.

The following subsections provide detailed information on the methodology used for designing both quantitative and qualitative experiments, including a description of the quantitative metrics, the structure of the selected questionnaire, the power analysis required to estimate the sample (number of total participants for the experiment) and the statistical analysis used to evaluate the collected data.

5.1 Quantitative Evaluation

Simulative Campaign The simulation campaign includes 180 simulations (trials) for each of the algorithms under consideration. The 180 trials consist of two distinct navigation scenarios: the first scenario, comprising 90 trials, involves three pedestrians, while the second scenario, comprising the remaining 90 trials, incorporates four pedestrians. Both scenarios are designed to replicate navigation situations characterized by low crowd density conditions, while simultaneously introducing a degree of variability in potential interactions between robots and pedestrians. In these scenarios, all pedestrians navigate from an initial position to a final destination using the SFM Gazebo's plugin. The deployment of this plugin is crucial for enabling simulated pedestrians to exhibit avoidance behaviors when encountering the robot, thereby enhancing the authenticity of assessments related to socially-aware navigation.

The simulation environment is created in Gazebo and characterized by the following dimensions: 8.5m x 5.5m. Thus, the overall area comprises approximately 47 m^2, which is consistent with the dimensions of environments commonly referenced in literature for conducting real-world experiments [10] [65]. Furthermore, this size closely aligns with the dimensions of the real room employed for testing the algorithms in a real-world context.

To guarantee that each simulation involves a minimum of one interaction between pedestrians and robot, the following methodology is adopted. First, the simulation environment is partitioned into six distinct fictitious zones, as shown in Fig. 7. Specifically, each fictitious zone z is defined by a set of coordinates ranges:

$$\begin{aligned} \boldsymbol{Z}_x &= \{x^z_{min}; x^z_{max}\} \\ \boldsymbol{Z}_y &= \{y^z_{min}; y^z_{max}\} \end{aligned} \tag{12}$$

Second, the spawn zones, denoting the simulation starting points, and the goal zones are strategically configured for each agent to guarantee the occurrence of interactions between agents, as summarized in Table 3.

For each trial, zone F is utilized to spawn the robot during its initialization within the simulated environment. On the

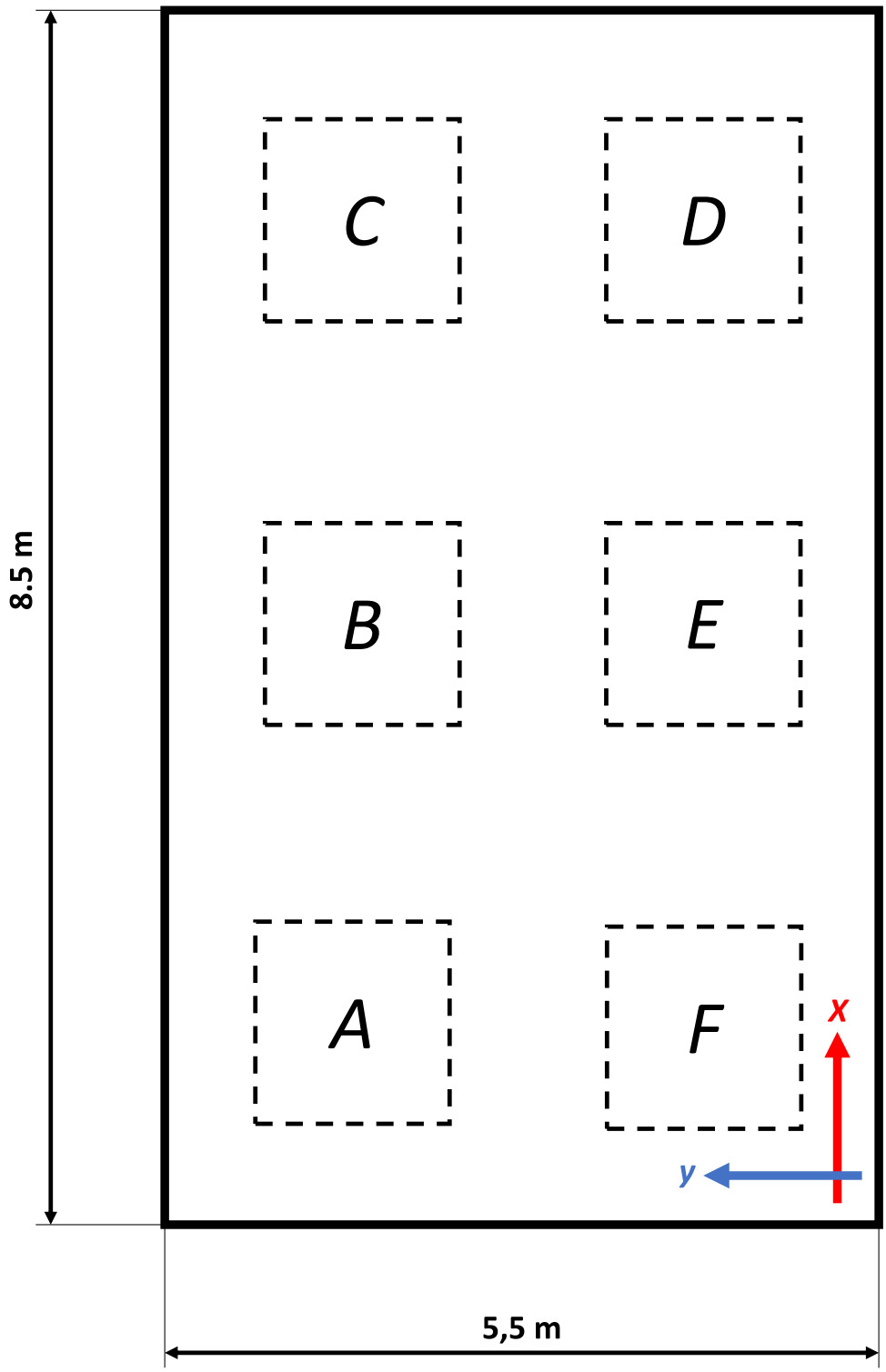


Fig. 7 Simulated environment with six fictitious zones

Table 3 Each spawn zone is paired with corresponding goal zones

Spawn zone	Goal zone
A	D, E
B	D, F
C	E, F
D	A, B
F	C

other hand, zones A, B, C, D are designated for the spawning of pedestrians.

Before the start of each trial, each pedestrian i, within the simulated environment, autonomously selects its spawn zone z from the available options, using a uniform distribution. Then, each pedestrian i stochastically determines its initial position within the chosen zone z, with the following equations:

$$x_i^z = x_{min}^z + rand(0, 10)\frac{x_{max}^z - x_{min}^z}{10} \tag{13}$$

$$y_i^z = y_{min}^z + rand(0, 10)\frac{y_{max}^z - y_{min}^z}{10} \tag{14}$$

where $rand(0, 10)$ is a uniformly distributed random number ranging from 0 to 10. Instead, x_{min}^z, x_{max}^z, y_{min}^z, y_{max}^z are the ranges of the chosen zone z.

The spawn zones are *mutually exclusive*, indicating that once a zone is chosen as a spawn location by one pedestrian, it becomes unavailable for selection by another pedestrian.

After determining its initial position, each pedestrian proceeds to randomly select the goal zone based on the principle outlined in Table 3. Subsequently, each pedestrian performs the calculation to determine the final goal position to reach within the chosen zone. This process is carried out using the same method employed for the calculation of initial position described in Eqs. 13 and 14. In this context as well, the chosen goal zones are *mutually exclusive* to prevent the occurrence of multiple pedestrians sharing a common target area.

Performance Metrics To enhance the robot's acceptance, navigation algorithms should ensure both their effectiveness in achieving goals and their ability to provide a natural and comfortable experience for humans. This necessitates the use of precise performance metrics that *quantitatively* assess these aspects. Several state-of-the-art performance metrics, such as those proposed by Biswas et al. [66] and Gao et al. [67], have been developed for this purpose. This section focuses on the chosen performance metrics adopted in this work to *quantitatively* evaluate different trajectories.

In particular, the performance metrics used to assess the trajectories' performance are:

Path Length Ratio (PLR):

This performance metric measures the ratio between the direct line-of-sight distance between the starting and ending points of a path, and the actual distance traversed by the agent between those two points:

$$PLR = \frac{\|\mathbf{p}_{robot}(T_{goal}) - \mathbf{p}_{robot}(0)|}{\sum_{t=1}^{T_{goal}} \|\mathbf{p}_{robot}(t) - \mathbf{p}_{robot}(t-1)\|} \tag{15}$$

where T_{goal} is the number of time-steps needed for the robot to reach its goal. Hence, this metric takes values in the range [0,1]. Generally, a high PLR is desirable, signifying that the agent tends to reach its destination while minimizing the length of the path. By measuring this metric, we can analyze how efficiently and successfully the agent navigates towards achieving its goal.

Average Speed (AS):

This metric represents the average speed of the agent along the entire trajectory, a factor used sometimes in evaluating its overall performance:

$$AS = \frac{\sum_{t=1}^{T_{goal}} \mathbf{v}_{robot}(t)}{T_{goal}} \tag{16}$$

However, this metric may also capture perceptions of *comfort*. Studies suggest a negative correlation between robot speed and perceived safety, potentially impacting comfort evaluations [68].

Closest Pedestrian Distance (CPD):

This metric denotes the distance between the agent i and the nearest agent j during the entire considered trajectory:

$$CPD = \min_{t,\, j} \|\mathbf{p}_{robot}(t) - \mathbf{p}_j(t)\| \tag{17}$$

An increased CPD value signifies that the agent i has a propensity to stay further away from the other agents. This contributes to increasing the level of *comfort* for humans.

Path Regularity (PR):

This metric evaluates *naturalness* by measuring the normalized rotations made by the agent during navigation. Such metric is computed as follows:

$$PR = 1 - \frac{\sum_{t=1}^{T_{goal}} |\theta(t) - \theta(t-1)|}{PI_{max}} \tag{18}$$

where $\theta(t)$ represents the robot's orientation at a generic time instant t and the denominator PI_{max} is the normalizing factor computed as:

$$PI_{max} = \max_{\substack{SFM,\\ ORCA,\\ GTSFM}} \sum_{t=1}^{T_{goal}} |\theta(t) - \theta(t-1)| \tag{19}$$

The PR assumes values within the range of [0,1]. A value of 1 signifies a direct path from the agent's starting point to the goal. On the other hand, a value approaching 0 indicates a significant number of rotations during navigation. For our purpose, it is preferred to obtain a PR value closer to 1, to have a smooth motion with few sudden changes in direction.

5.2 Qualitative Evaluation

Real-world Experiments The room of the real-world experiment is approximately 40 m^2. The involved participants are 2 and one robot (Locobot WX250). The total number of participants was 76, exceeding the minimum sample estimated with the power analysis presented in the paragraph below. Within the experiment, every participant is assigned a specific starting point and a corresponding goal to achieve.

The experimental protocol comprises **three phases**:

1. **Explanation of the experiment and collection of participant general information**
   In this phase, each participant receives detailed information regarding the research objectives, experimental procedure, risks and benefits of the experiment, and the right to withdraw at any time from the experiment. Additionally, each participant is given a consent form to sign, granting their participation in the research project. Then, the participants are required to provide their gender, age, and level of experience in the robotics field on a Likert scale from 1 (no experience) to 5 (expert). This phase is expected to take about 6 minutes;
2. **Participant training**
   During this phase, participants are allowed to walk in the room for 3 minutes without the robot. Subsequently, participants have another 3 minutes to walk in the same room but with the robot. This phase is essential to allow each participant to become familiar with the environment and the experiment scenario;
3. **Experiment**
   In this phase, participants walk from a predefined starting point to a goal. This phase will consist of *3 sessions*, one for each algorithm. Within each session, *4 trials* are conducted. At the end of each session, each participant completes an online questionnaire based on the Human-Robot Interaction Evaluation Scale (HRIES scale [64]).

The order of the sessions for each experiment is randomized to avoid collecting data with biases related to the order of execution of the different algorithms. Each session is expected to take about 5 minutes. To complete the entire experiment, each participant needs approximately **30 minutes**.

Items	Factor
Warm	Sociability
Likeable	Sociability
Trustworthy	Sociability
Friendly	Sociability
Alive	Animacy
Natural	Animacy
Real	Animacy
Human-like	Animacy
Self-reliant	Agency
Rational	Agency
Intentional	Agency
Intelligent	Agency
Creepy	Disturbance
Scary	Disturbance
Uncanny	Disturbance
Weird	Disturbance

Fig. 8 The Human-Robot Interaction Evaluation Scale (HRIES) [64]

Survey Questionnaire

To evaluate how humans perceive robots controlled by the GTSFM algorithm, the HRIES is adopted.

Figure 8 illustrates the scale developed in [64]. The scale is designed to assess how humans perceive robots, with a particular focus on *anthropomorphism*. However, the concept of anthropomorphism is too broad to be measured directly. Therefore, the authors identify four *factors* (shown on the right in Fig. 8) that are measured through *items* (depicted on the left in Fig. 8).

The *factors* on the scale are: sociability, animacy, agency, and disturbance. Sociability is characterized by the capacity of an individual or group to interact effectively and with positive engagement with others. The animacy suggests human characteristics for non-human agents. The agency is the capacity of a robot to act independently and make its own decisions, thus is strictly linked with the perceived intelligence of the robot. The disturbance captures the negative valence associated with perceptions of robot, including feelings of discomfort and specific negative evaluations.

The questionnaire is available in English and Italian, allowing participants to choose the language they feel most comfortable with. The Italian translation of the HRIES scale is presented in Table 4. The translation of the *items* is conducted with the assistance of the scale author, Dr. Spatola.

Regarding the practical use of the scale, we follow the instructions reported in [64], tailoring the research question to align with the robotic behavior of interest: the robot's movement. In particular, each item is rated using a 7-point Likert scale, answering the following question:

"Using the provided scale, how closely are the words below associated with the robot's motion during the experiment?"

Table 4 Italian translation of the items in HRIES

Items in English	Items in Italian
Warm	Caloroso
Likeable	Piacevole
Trustworthy	Affidabile
Friendly	Amichevole
Alive	Vivo
Natural	Naturale
Real	Reale
Human-like	Sembianze umane
Self-reliant	Autonomo
Rational	Razionale
Intentional	Intenzionale
Intelligent	Intelligente
Creepy	Raccapricciante
Scary	Spaventoso
Uncanny	Inquietante
Weird	Strano

By collecting data on the anthropomorphization of the robot's behavior, we collect information about how humans perceive the robot. Specifically, the algorithm that is perceived with the highest anthropomorphism probably shares more human-like characteristics than the other algorithms, being the most socially accepted [33].

A Priori Power Analysis Our study aims to investigate the subjective perception of the GTSFM algorithm in comparison to SFM and ORCA algorithms. To estimate the number of participants ensuring the reliability and validity of our findings [69], we conducted a rigorous a-priori power analysis, employing the freely available software G*Power [70]. The HRIES questionnaire, chosen in our study for the real-world experiment, is validated through different studies in [64], where a normal distribution of data is assumed. Based on these previous studies, we also assumed that our data adhere to a normal distribution. Consequently, this allows us to confidently support the use of parametric tests in our analysis [71]. Then, we assumed that the data collected during the real-world experiment can be analyzed via the parametric one-way ANOVA because our independent variables are more than two independent groups (GTSFM, SFM and ORCA) and our dependent variables (the factors of the questionnaire) are continuous since the factors are computed through the Principal Component Analysis [72]. The result of the a-priori analysis for the one-way ANOVA was 66 volunteers, considering an alpha level equal to 5%, power of the study 80% and the three groups, corresponding to the three different algorithms. We recruited the participants using the Institutional email of Politecnico di Torino and then, we invited them to come to the lab, where the experiment took place. Ultimately, we collected 76 responses, exceeding the sample size of 66.

Statistical Analysis of Data The objective of the statistical data analysis of the *qualitative* data is to reject the following null hypothesis:

All algorithms (GTSFM, SFM, ORCA) are perceived by participants as indistinguishable.

To achieve this objective, first of all, it is necessary to reduce the dimension of the dataset from the items to the possible factors through the principal component analysis (PCA) [72]. Before performing the PCA analysis, the merging of the data collected for each algorithm is necessary, since the PCA requires a single dataset of all the data collected. Then, to ensure that all items have the same scale, the standardization of the data is performed. Subsequently, the PCA is performed and the loadings are rotated. The rotation of the loadings is a post-processing step that can improve the interpretability of the results by making the loadings more meaningful [72]. Finally, the *score* of each principal component for each participant is computed, considering the linear combination of the standardized data with the computed loadings.

Then, to reject the null hypothesis, the one-way ANOVA is performed on the computed *score*. If the one-way ANOVA test produces a statistical significance value (p-value) below 5%, it means there is the presence of at least one group that has a significant difference from the others in terms of some factor. To discover which groups are classified as significantly different, a post-hoc analysis is performed considering two pairs of groups at a time.

6 Results

6.1 Quantitative Results

The outcomes of the performance metrics, obtained through a Monte Carlo numerical simulation, are shown in Fig. 9.

For each performance metric, a Kruskal-Wallis test is conducted to statistically reject the following null hypothesis:

Null Hypotesis All algorithms (GTSFM, SFM, ORCA) are statistically indistinguishable considering the state-of-the-art performance metrics testing social navigation.

Then, since for each performance metric, a statistically significant difference is identified ($p < 0.05$, $\chi^2 = 173,22$ for PLR; $p < 0.05$, $\chi^2 = 222,00$ for AS; $p < 0.05$, $\chi^2 = 53,18$ for CPD; $p < 0.05$, $\chi^2 = 435,16$ for PR), a post-hoc analysis, involving pairwise comparison of algorithms, is conducted and below is discussed.

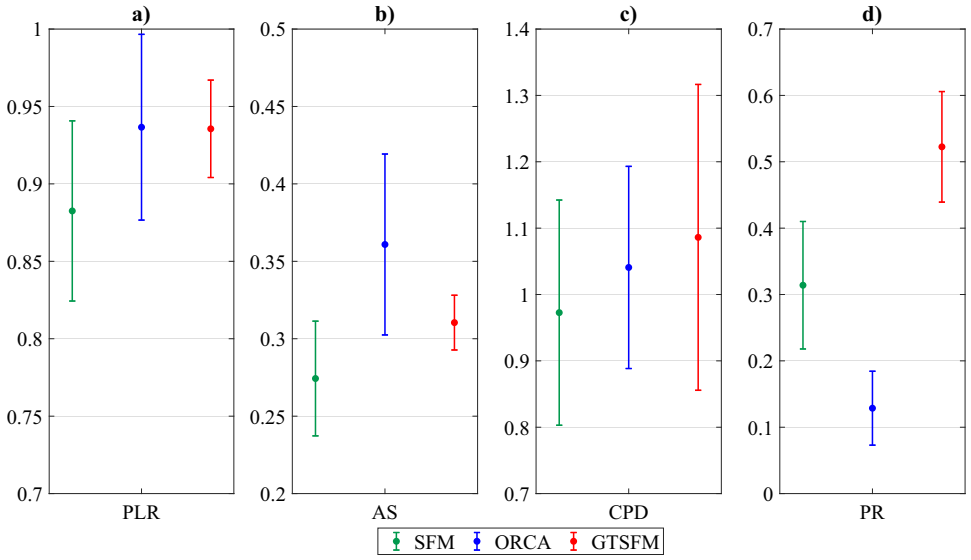


Fig. 9 Mean value and standard deviation of the considered performance metrics for each algorithm: SFM (Social Force Model), ORCA (Optimal Reciprocal Collision Avoidance), GTSFM (Game-theoretic Social Force Model). The performance metrics are: a) PLR (Path Length Ratio), b) AS (Average Speed), c) CPD (Closest Pedestrian Distance), d) PR (Path Regularity)

In general, our numerical validation confirms that GTSFM exhibits a significant improvement over SFM across all four performance metrics.

In particular, in Fig. 9a, the PLR for each algorithm is shown and reveals that the SFM is characterized by the lowest average PLR, followed by ORCA and GTSFM in a tie. Although ORCA has a very similar mean value to GTSFM, post-hoc analysis reveals a presence of significant statistical difference ($p = 0.02$). This result is justified by the fact that the post-hoc analysis compares the mean of the calculated ranks and not the mean of the values (mean rank SFM= 148,11; mean rank ORCA=353.59; mean rank GTSFM=309.79). When examining the remaining pairs of groups, a statistically significant difference is observed (SFM-ORCA $p < 0.05$; SFM-GTSFM $p < 0.05$). Regarding the standard deviation, ORCA and SFM exhibit a higher variability than GTSFM. This result indicates that in terms of PLR, the repeatability and predictability of each experimental condition are much higher in GTSFM than in ORCA and SFM.

The average speed (AS) in the three experimental conditions is illustrated in Fig. 9b, where the highest average value is related to ORCA, followed by GTSFM and SFM, which are in turn distinguishable from one another (post-hoc analysis: for SFM-ORCA $p < 0.05$; for SFM-GTSFM $p < 0.05$; for ORCA-GTSFM $p < 0.05$). The highest mean value of ORCA is justified by the fact that ORCA is designed to maximize the velocity of the robot maintaining a safe distance from other agents. GTSFM maintains a higher mean value than SFM because one of the distinctive features of GTSFM lies in its predictive logic. Unlike SFM, which tends to avoid agents when it is nearby, GTSFM adopts a strategy of reducing speed and selecting a trajectory that avoids people in advance. Similar to SFM, ORCA is a reactive method and thus fails to predict the trajectories of other agents along a consistent time horizon. This limitation results in higher standard deviations for ORCA and SFM compared to GTSFM, suggesting their potential for less stable navigation in dynamic environments. This result highlights the fact that the average speed of the GTSFM remains about the same in the 180 trial indicating a greater repeatability capacity of the GTSFM than the other two algorithms.

Although the results are promising, the average speed values obtained are not yet comparable to human speed values. This limitation is tied to the physical constraints of the Locobot, which has a maximum speed limit of 0.5 m/s.

Average values of CPD in the three experimental conditions are illustrated in Fig. 9c, where the highest average value is related to GTSFM, followed by ORCA and SFM. The reason for this ranking is presumably due to the purely reactive design of the ORCA and SFM algorithm. Although GTSFM has a higher mean value than ORCA, post-hoc analysis reveals an absence of significant statistical difference ($p = 0.79$), proving that both algorithms try to maintain a certain distance from people to ensure their comfort. When examining the remaining pairs of groups, a statistically significant difference is observed (SFM-ORCA $p < 0.05$; SFM-GTSFM $p < 0.05$).

The metric that most clearly underlines the significant advantage of employing game theory in navigation is path regularity (PR). In Fig. 9d, the average PR for each experimental condition is illustrated, where the highest average value pertains to GTSFM, followed by SFM and ORCA, each of which is distinguishable from the others (post-hoc analysis: for SFM-ORCA $p < 0.05$; for SFM-GTSFM $p < 0.05$; for ORCA-GTSFM $p < 0.05$). The highest mean value of the GTSFM is probably justified by the incorporation of game theory enables the identification of optimal parameters within

Table 5 Demographic characteristics and participants' levels of experience with robotics, assessed on a scale ranging from 1 (indicating minimal experience) to 5 (indicating maximal experience)

Number of Participants	76
Gender	Male 73.7% and Female 26.3%
Age	24.99 ± 3.91
Experience with robotics	2.03 ± 1.07

This data is gathered in the first phase of the experiment

the SFM to execute evasive maneuvers as smoothly as possible.

6.2 Qualitative Results

We collected 76 responses for the real-world experiment, where the average age of the participants was approximately 25, having limited robotics experience. The gender composition is unbalanced toward men (Table 5).

Firstly, experimental outcomes are analyzed with the PCA to reduce the dimension of the dataset through the identification of the latent factors. Then, the one-way ANOVA is performed to statistically reject the following null hypothesis.

Our null hypothesis posits: *All algorithms (GTSFM, SFM, ORCA) are perceived by participants as indistinguishable.*

A summary of the PCA loadings for each item is presented in Fig. 10. The latter highlights the four main components that exhibit the highest variances to try to interpret each component with the factor of the HRIES scale. However, as can be easily deduced from the Fig. 10, only the first two components can be directly associated with two factors of the scale. The remaining two factors do not align significantly with any of the PCA components. In particular, the first component exhibits a significant concentration of items associated with *agency*, while also displaying a moderate influence from *animacy* and *sociability*. The second component predominantly comprises items associated with *disturbance*. Nevertheless, the lack of interpretability for the remaining two components associated with *sociability* and *animacy* factors might be attributed to the non-human appearance of the robot, which precludes reliable assessments for these factors.

Means and standard deviations of component scores are presented in Fig. 11. Specifically, the measure of the perceived *agency* across the three algorithms is illustrated in Fig. 11a, where the SFM is characterized by the highest average score, followed by GTSFM and ORCA. However, despite the initial indications of the one-way ANOVA ($F = 4.54$, $p = 0.01$) of significant differences in agency scores among the algorithms, a post-hoc analysis (Table 6) reveals that only the pair SFM-ORCA is statistically different. Participants perceive the remaining pairs as being indistinguishable.

On the other hand, the measure of the perceived *disturbance* across the same algorithms is illustrated in Fig. 11b, where ORCA is characterized by the highest average score, followed by GTSFM and SFM. Nevertheless, the one-way ANOVA, conducted on disturbance scores, reveals the absence of statistically significant differences ($F = 0.67$, $p = 0.51$). These findings indicate that participants are unable to detect differences in comfort between the three algorithms.

7 Discussion and conclusions

This study aims to develop a navigation system that generates trajectories for autonomous robots to ensure the social acceptance of humans by leveraging the concept of anthropomorphism.

To achieve this goal, we combined the well-known Social Force Model with game theory (GTSFM) to devise a trajectory planning algorithm. This algorithm enables the robot to anticipate human movements and navigate smoothly.

Fig. 10 Loadings for each item considering 4 principal components as suggested by the HRIES scale [64]. In bold is highlighted the maximum value for each item. Highlighted in yellow are the items that make the most significant contributions to that component

Latent factor	Item	1st Component	2nd Component	3rd Component	4th Component
Sociability	Warm	-0,0588	**0,0200**	-0,5046	-0,0033
Sociability	Likeable	**0,0105**	-0,0224	-0,2807	-0,2751
Sociability	Trustworthy	**0,2358**	-0,1018	-0,1567	-0,0793
Sociability	Friendly	0,0561	-0,1098	-0,5934	**0,1916**
Animacy	Alive	**0,1870**	0,1652	-0,2116	-0,1057
Animacy	Natural	-0,0224	**0,0741**	-0,1025	-0,4938
Animacy	Real	**0,2165**	0,0325	-0,0163	-0,2919
Animacy	Human-like	-0,0359	**0,0642**	-0,3922	-0,1257
Agency	Self-Reliant	**0,6017**	-0,0831	-0,0042	0,2245
Agency	Rational	**0,4628**	-0,0189	0,0080	-0,0032
Agency	Intentional	**0,4327**	0,0812	0,1757	-0,1421
Agency	Intelligent	**0,2469**	0,0565	-0,0083	-0,3085
Disturbance	Creepy	-0,0589	**0,5444**	0,0289	-0,0125
Disturbance	Scary	0,0562	**0,5741**	0,1091	-0,0366
Disturbance	Uncanny	-0,0477	**0,4997**	-0,1532	0,0520
Disturbance	Weird	0,1441	0,2145	-0,1157	**0,5961**
Percentage of explained variance		41,33%	16,95%	7,18%	4,89%

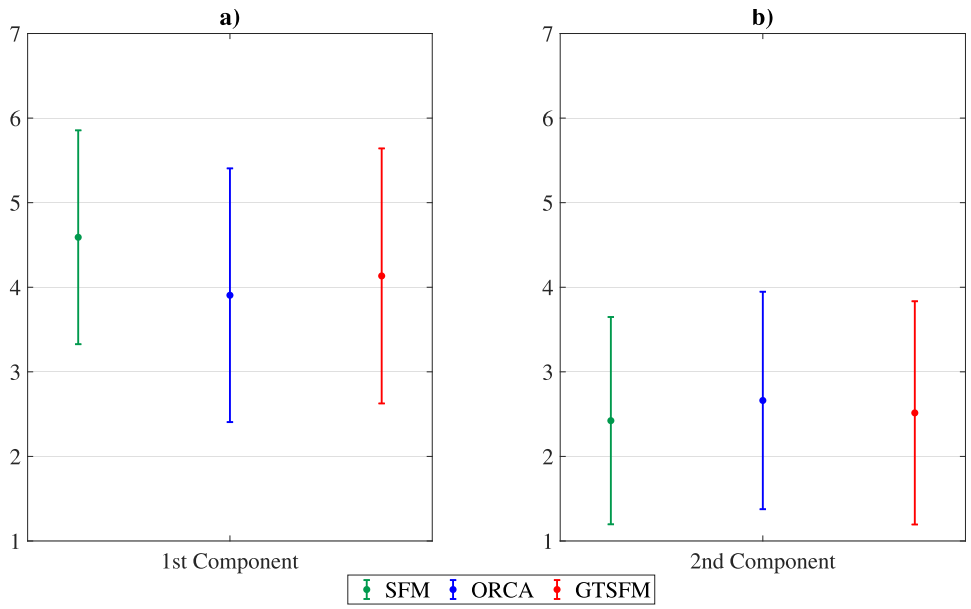


Fig. 11 Mean and standard deviation of component scores across different algorithms: SFM (Social Force Model), ORCA (Optimal Reciprocal Collision Avoidance), GTSFM (Game-theoretic Social Force Model). The components are: a) 1st Component is the perceived *agency*, b) 2nd Component is the perceived *disturbance*

To assess the social acceptability of the generated robotic trajectories, we conducted a twofold validation: first, we evaluated *quantitatively* the performance of the generated trajectories across three experimental conditions (SFM, ORCA and GTSFM) through performance parameters of the state of the art (PLR, AS, CPD, and PR). This validation has been done through a Monte Carlo simulation campaign. Then, we performed a *qualitative* analysis through a survey questionnaire with a statistically significant group of volunteers using the HRIES scale [64]. This validation has been done through a real-world experiment.

The most significant finding of the *quantitative* analysis is that the GTSFM algorithm produces smoother paths than the two state-of-the-art algorithms, resulting in a more natural motion. Moreover, through numerical validation, we have consistently observed that GTSFM outperforms SFM across the four performance metrics. In particular, the results suggest that GTSFM excels in finding shorter, smoother paths with a higher speed than SFM, reducing the time to reach the goal while maintaining a safer distance from humans. This finding highlights the effectiveness of GTSFM in achieving more efficient and natural navigation compared to SFM.

Table 6 Post-Hoc analysis on the score of the 1st component

Algorithm 1	Algorithm 2	p-value
SFM	ORCA	0.009
SFM	GTSFM	0.119
ORCA	GTSFM	0.586

In yellow is highlighted the statistically different pair

While ORCA excels in speed (AS) and efficiency (PLR), its social navigation capabilities are lower than GTSFM. Indeed, ORCA's trajectories tend to be less smooth and closer to pedestrians than GTSFM, potentially increasing the risk of collisions and pedestrian disturbance.

Nevertheless, these *quantitative* findings are not consistent with the *qualitative* results. The latter reveals that none of the considered principal components shows a statistically significant difference between the algorithms, except for SFM and ORCA in the case of agency (the first component). This apparent contradiction between the two types of analysis raises interesting questions about the reasons behind these findings. This discrepancy could potentially stem from the influence of unaccounted factors. One such factor might be the robot's appearance, which obscures the distinction between the algorithms. Additionally, the limited maximum velocity of the real robot (0.5 m/s) compared to the average human walking velocity (1.4 m/s [73]) might have hindered the identification of a potentially anthropomorphic algorithm.

Algorithm acceptability is evaluated through both *quantitative* and *qualitative* measures, each addressing distinct aspects. Nonetheless, some measures aim to understand shared underlying factors, allowing for a unified discussion of these measures.

Quantitative measures, such as PLR, AS, CPD, and PR, provide objective assessments of algorithm performance. PLR indicates the overall efficiency of the algorithm, while AS and CPD measure how comfortable the generated trajectories are for humans. In particular, the human comfort decreases as the robot's speed of movement increases [68]. Instead, the human comfort increases as the robot's distance from humans increases [68]. PR assesses the smoothness of

the trajectories, which is related to the naturalness of the robot's movements [67].

On the other hand, the *qualitative* measurement based on the HRIES scale, focuses on the anthropomorphism of the robot's motion. These measures include sociability, animacy, agency, and disturbance. We choose the HRIES because, unlike the state of the art [74, 75], the authors in [64] developed the HRIES using different types of robots (not just humanoids), making the scale generalizable to all types of robots. Additionally, unlike other scales that validate the questionnaire with static images [75], the authors in [64] validate the scale by conducting tests with robots in motion (via videos). Furthermore, the authors in [64] also conduct a test with a real robot to further assess the validity of the scale. Since, for conducting the real-world experiment, we use a non-humanoid robot that navigates and shares the environment with humans, the aforementioned scale is particularly well-suited for our case.

Building upon this explanation, further insight can be gained by bridging the gap between *quantitative* and *qualitative* results. This can be achieved by analyzing the relationship between objective measurements like AS and CPD with the subjective evaluation of perceived *disturbance* captured by the HRIES scale.

Considering the AS, the ORCA algorithm has the highest average speed value which turns out to be the one with the highest perceived disturbance among the three algorithms, although there is no statistical difference across the considered algorithms. This statistical indistinguishability between the algorithms may be attributed to the limitations of the robot's velocity (0.5 m/s). While the ORCA algorithm might theoretically promote faster movements compared to other algorithms, the robot's hardware limitations restrict its maximum achievable velocity. This velocity may be insufficient to elicit feelings of discomfort in human subjects which may lead to the absence of an identification of a statistically significant difference between the algorithms.

While the GTSFM exhibits a greater average CPD than SFM, real-world experiments do not translate this objective metric into a higher perceived comfort for GTSFM than SFM. This discrepancy can be explained by considering the different contexts in which the measurements have been taken. *Quantitative* measurements have been conducted in a simulated environment, where pedestrians have exhibited rational movements and have interacted with the robot as another human in a shared space. In contrast, the real-world experiment shows that despite the robot being programmed to maintain a specific distance, participants tend to approach closer than they would with a real person (maybe for curiosity reasons), thereby obscuring the distinctions between the different algorithms

Another potential comparison between *quantitative* and *qualitative* analyses can be made by correlating PR measurements with the evaluation of *animacy*. This comparison is justified because when a robot exhibits smooth movements, it resembles the typical non-nervous motions of humans. Thus, the robot is perceived as more human-like [67]. Unfortunately, this comparison cannot be made since, after the PCA, the *animacy* cannot be uniquely attributed to any of the identified components, thus failing to be interpreted and discussed. We have encountered a similar challenge regarding *sociability*, as we cannot unequivocally attribute a principal component to this factor.

We have reason to believe that probably these two problems are caused by the robot's appearance. Although the questions are about the robot's movement, it is impossible to completely separate the robot's movement from its appearance. This makes the measures of *animacy* and *sociability* unreliable for further discussion.

These findings are consistent with other studies in literature [33, 76], where the authors shows that the physical appearance of a robot plays a significant role in shaping how people perceive and interact with it. This highlights the importance of considering the appearance of a robot when developing a socially-aware robot algorithm. Moreover, in [77], authors have investigated how the appearance and movement characteristics of a robot can influence people's perceptions of its animacy. The main result of the study in [77] is: when the robot has a human-like appearance, humans perceive naturalistic motion as more animate compared to mechanical motion. This difference is not perceived when the robot lacks human-like appearance. This finding aligns with our results on animacy, where we observed *quantitative* differences between algorithms but no *qualitative* distinctions.

When interpreting the results of our study, we should also acknowledge the limitations of the *quantitative* and *qualitative* validation. Regarding the former, it has been conducted in a simulated environment where humans have been not real people but rather controlled by a human motion model. This model has been used to simulate various human behaviors by adjusting different parameters. However, this approach has two limitations: first, it does not explicitly model the stochastic nature of human behavior, even though this is implicitly accounted through parameter tuning. Second, it is not possible to accurately assess real human-robot interaction, as humans simply avoid the robot as another peer human in the simulation.

On the other hand, one of the main limitations of the *qualitative* validation lies in the constrained movement speed imposed upon the participants. This artificial restriction has been necessary to ensure interaction with the robot, as its maximum speed is 0.5 m/s. Furthermore, such restricted speed of the robot may have limited the range of conditions tested among the different experimental conditions and consequently, the ability to comprehensively assess perceived comfort in human subjects.

The non-humanoid appearance of the robot and its relatively small size likely have contributed to limitations in measuring sociability and animacy. Moreover, during the experiment, participants have not been engaged in a peer-to-peer interaction with the robot, instead assuming a leader-follower interaction. This phenomenon could be attributed to the robot's non-humanoid characteristics, such as the absence of a face, two arms and a typical body structure. Additionally, the robot's height of 63 cm, significantly below the Italian average height of humans (1.68 m [78]), contributes to an appearance reminiscent of a toy-like aesthetic. This lack of human-like features may have hindered the development of a peer-to-peer rapport.

Throughout the experiment, participants consistently approached the robot more closely than they did other humans. This behavior may be attributed to either the participants' natural curiosity or the perceived non-threatening nature of the robot, possibly influenced by its small size.

Our work can be extended in several directions.

To make the *quantitative* analysis as realistic and precise as possible, a real experiment should be created by placing the robot in a real environment (such as a corridor in a hospital or at university). In this way, we would have real people interacting with the robot, rather than agents simulated by models. In this ideal test, reliable data could also be collected about human-robot interaction (as people would feel free without the constraints and biases of laboratory experiments). This approach would allow us to collect more realistic data than our simulated data. Furthermore, this approach could help to understand the type of interaction between humans and robot, whether it is a peer-to-peer or leader-follower interaction.

Regarding the *qualitative* analysis, we believe that the experiment protocol is reliable and the biggest limitations were the limited robot's speed and its appearance. Therefore, we recommend repeating the experiment proposed in this study, choosing a robot that has a speed comparable to humans (1.4 m/s [73]). In addition, the author in [33] showed that in evaluating how human-like a robot appears, the robot's head and face receive considerable attention, since this body part is crucial in human-human communication. Therefore, we recommend a robot that has this body part. The choice of the robot's height is also essential [79]. For this reason, a robot with a height very similar to humans (1.68 m) should be chosen.

The main result of this study is that probably the choice of the robot is essential to ensure an interaction as similar as possible to that of humans to obtain statistically significant results even at the level of motion measurement.

Author Contributions All authors contributed to the formal analysis, investigation, methodology, and validation of the study. Data curation was performed by Giada Galati. Software design and data visualization were performed by Giada Galati, Andrea Usai and Giacomo Vignolo. Alessandro Rizzo handled Funding Acquisition, Project Administration, and Resources. Supervision was provided by Alessandro Rizzo and Simone Macrì. The first draft of the manuscript was written by Giada Galati, Andrea Usai and Giacomo Vignolo and all authors commented on previous versions of the manuscript. All authors read, edited, and approved the final version of the manuscript.

Funding Open access funding provided by Politecnico di Torino within the CRUI-CARE Agreement. This study was carried out within the FAIR - Future Artificial Intelligence Research and received funding from the European Union Next-GenerationEU (PIANO NAZIONALE DI RIPRESA E RESILIENZA (PNRR) – MISSIONE 4 COMPONENTE 2, INVESTIMENTO 1.3 – D.D. 1555 11/10/2022, PE00000013). It was also carried within the MOST – Sustainable Mobility National Research Center and received funding from the European Union Next-GenerationEU (PIANO NAZIONALE DI RIPRESA E RESILIENZA (PNRR) – MISSIONE 4 COMPONENTE 2, INVESTIMENTO 1.4 – D.D. 1033 17/06/2022, CN00000023). This manuscript reflects only the authors' views and opinions, neither the European Union nor the European Commission can be considered responsible for them.

Data Availability The data associated with the qualitative evaluation will be made available upon reasonable request.

Declarations

Competing Interests Alessandro Rizzo is a Senior Editor at Large of the Journal of Intelligent and Robotic Systems. The authors declare no additional conflicts of interest.

Ethics approval The experiment protocol received ethical approval (protocol number: 90584/2023) from the Politecnico di Torino's ethics committee.

Consent to participate Informed consent was obtained from all individual participants included in the study.

Consent to publish The authors affirm that human research participants provided informed consent for publication of the image in Figure 3.

Open Access This article is licensed under a Creative Commons Attribution 4.0 International License, which permits use, sharing, adaptation, distribution and reproduction in any medium or format, as long as you give appropriate credit to the original author(s) and the source, provide a link to the Creative Commons licence, and indicate if changes were made. The images or other third party material in this article are included in the article's Creative Commons licence, unless indicated otherwise in a credit line to the material. If material is not included in the article's Creative Commons licence and your intended use is not permitted by statutory regulation or exceeds the permitted use, you will need to obtain permission directly from the copyright holder. To view a copy of this licence, visit http://creativecommons.org/licenses/by/4.0/.

References

1. Hellou, M., Lim, J., Gasteiger, N., Jang, M., Ahn, H.S.: Technical methods for social robots in museum settings: an overview of the literature. Int. J. Soc. Robot. **14**(8), 1767–1786 (2022)
2. Zhao, Z., Chen, W., Peter, C.C. , Wu, X.: A novel navigation system for indoor cleaning robot. In: 2016 IEEE international conference

on Robotics and Biomimetics (ROBIO), pp. 2159–2164. IEEE (2016)
3. Takahashi, M., Suzuki, T., Shitamoto, H., Moriguchi, T., Yoshida, K.: Developing a mobile robot for transport applications in the hospital domain. Robot. Auton. Syst. **58**(7), 889–899 (2010)
4. Kümmerle, R., Ruhnke, M., Steder, B., Stachniss, C., Burgard, W.: Autonomous robot navigation in highly populated pedestrian zones. J. Field Robot. **32**(4), 565–589 (2015)
5. Araujo, A.R., Caminhas, D.D., Pereira, G.A.: An architecture for navigation of service robots in human-populated office-like environments. IFAC-PapersOnLine **48**(19), 189–194 (2015)
6. Kruse, T., Pandey, A.K., Alami, R., Kirsch, A.: Human-aware robot navigation: a survey. Robot. Auton. Syst. **61**(12), 1726–1743 (2013)
7. Hewawasam, H., Ibrahim, M.Y., Appuhamillage, G.K.: Past, present and future of path-planning algorithms for mobile robot navigation in dynamic environments. IEEE Open J. Ind. Electron. Soc. **3**, 353–365 (2022)
8. Kivrak, H., Cakmak, F., Kose, H., Yavuz, S.: Social navigation framework for assistive robots in human inhabited unknown environments. Eng. Sci. Technol. Int J. 100 (2020)
9. Trautman, P., Ma, J., Murray, R.M., Krause, A.: Robot navigation in dense human crowds: statistical models and experimental studies of human-robot cooperation. Int. J. Robot. Res. **34**(3), 335–356 (2015)
10. Turnwald, A., Wollherr, D.: Human-like motion planning based on game theoretic decision making. Int. J. Soc. Robot. **11**, 151–170 (2019)
11. Sisbot, E.A., Marin-Urias, L.F., Alami, R., Simeon, T.: A human aware mobile robot motion planner. IEEE Trans. Rob. **23**(5), 874–883 (2007)
12. Shiomi, M., Zanlungo, F., Hayashi, K., Kanda, T.: Towards a socially acceptable collision avoidance for a mobile robot navigating among pedestrians using a pedestrian model. Int. J. Soc. Robot. **6**(3), 443–455 (2014)
13. Chen, Y.F., Everett, M., Liu, M., How, J. P.: Socially aware motion planning with deep reinforcement learning. In: 2017 IEEE/RSJ International Conference on Intelligent Robots and Systems (IROS), pp. 1343–1350. IEEE (2017)
14. Nash, J.: Non-cooperative games. Ann. Math. 286–295 (1951)
15. Quijano, N., et al.: The role of population games and evolutionary dynamics in distributed control systems: the advantages of evolutionary game theory. IEEE Control Syst. Mag. **37**(1), 70–97 (2017)
16. Ye, M., Zino, L., Rizzo, A., Cao, M.: Game-theoretic modeling of collective decision making during epidemics. Phys. Rev. E **104**(2), 024314 (2021)
17. Tanimoto, J., Hagishima, A., Tanaka, Y.: Study of bottleneck effect at an emergency evacuation exit using cellular automata model, mean field approximation analysis, and game theory. XXPhys. A **389**(24), 5611–5618 (2010)
18. Mesmer, B.L., Bloebaum, C.L.: Modeling decision and game theory based pedestrian velocity vector decisions with interacting individuals. Saf. Sci. **87**, 116–130 (2016)
19. Rahmati, Y., Talebpour, A., Mittal, A., Fishelson, J.: Game theory-based framework for modeling human-vehicle interactions on the road. Transp. Res. Rec. **2674**(9), 701–713 (2020)
20. Kim, C., Won, J.-S.: A fuzzy analytic hierarchy process and cooperative game theory combined multiple mobile robot navigation algorithm. Sensors **20**(10), 2827 (2020)
21. LaValle, S. M., Hutchinson, S.: Game theory as a unifying structure for a variety of robot tasks. In: Proceedings of 8th IEEE international symposium on intelligent control, pp. 429–434. IEEE (1993)
22. Meng, Y.: Multi-robot searching using game-theory based approach. Int. J. Adv. Rob. Syst. **5**(4), 44 (2008)
23. Helbing, D., Molnar, P.: Social force model for pedestrian dynamics. Phys. Rev. E **51**(5), 4282 (1995)
24. Tadokoro, S., Hayashi, M., Manabe, Y., Nakami, Y., Takamori, T.: On motion planning of mobile robots which coexist and cooperate with human. In: Proceedings 1995 IEEE/RSJ International Conference on Intelligent Robots and Systems. Human Robot Interaction and Cooperative Robots, vol. 2, pp. 518–523. IEEE (1995)
25. Hoeller, F., Schulz, D., Moors, M., Schneider, F. E.: Accompanying persons with a mobile robot using motion prediction and probabilistic roadmaps. In: 2007 IEEE/RSJ international conference on intelligent robots and systems, pp. 1260–1265. IEEE (2007)
26. Bennewitz, M., Burgard, W., Cielniak, G., Thrun, S.: Learning motion patterns of people for compliant robot motion. Int. J. Robot. Res. **24**(1), 31–48 (2005)
27. Alahi, A., Goel, K., Ramanathan, V., Robicquet, A., Fei-Fei, L., Savarese, S.: Social lstm: human trajectory prediction in crowded spaces. In: Proceedings of the IEEE conference on computer vision and pattern recognition, pp. 961–971. (2016)
28. Gupta, A., Johnson, J., Fei-Fei, L., Savarese, S., Alahi, A.: Social gan: Socially acceptable trajectories with generative adversarial networks. In: Proceedings of the IEEE conference on computer vision and pattern recognition, pp. 2255–2264. (2018)
29. Liang, J., Jiang, L., Niebles, J. C., Hauptmann, A. G. , Fei-Fei, L.: Peeking into the future: predicting future person activities and locations in videos. In: Proceedings of the IEEE conference on computer vision and pattern recognition, pp. 5725–5734. (2019)
30. Turnwald, A., Althoff, D., Wollherr, D., Buss, M.: Understanding human avoidance behavior: interaction-aware decision making based on game theory. Int. J. Soc. Robot. **8**(2), 331–351 (2016)
31. Das, S., Suganthan, P.N.: Differential evolution: a survey of the state-of-the-art. IEEE Trans. Evol. Comput. **15**(1), 4–31 (2010)
32. Waytz, A., Cacioppo, J., Epley, N.: Who sees human? the stability and importance of individual differences in anthropomorphism. Perspect. Psychol. Sci. **5**(3), 219–232 (2010)
33. Fink, J.: Anthropomorphism and human likeness in the design of robots and human-robot interaction. In: International conference on social robotics, pp. 199–208. Springer (2012)
34. Van Den Berg, J., Guy, S. J., Lin, M., Manocha, D.: Reciprocal n-body collision avoidance. In: Robotics Research: The 14th International Symposium ISRR, pp. 3–19. Springer (2011)
35. Antonucci, A., et al.: Socially aware robot navigation. Tesi di dottorato. (2022)
36. Ratsamee, P., Mae, Y., Kamiyama, K., Horade, M., Kojima, M., Arai, T.: Social interactive robot navigation based on human intention analysis from face orientation and human path prediction. Robomech J. **2**(1), 1–18 (2015)
37. Ferrer, G., Zulueta, A.G., Cotarelo, F.H., Sanfeliu, A.: Robot social-aware navigation framework to accompany people walking side-by-side. Auton. Robot. **41**(4), 775–793 (2017)
38. Fiorini, P., Shiller, Z.: Motion planning in dynamic environments using velocity obstacles. Int. J. Robot. Res. **17**(7), 760–772 (1998)
39. Van den Berg, J., Lin, M., Manocha, D.: Reciprocal velocity obstacles for real-time multi-agent navigation. In: 2008 IEEE international conference on robotics and automation, pp. 1928–1935. IEEE (2008)
40. Galati, G., Primatesta, S., Grammatico, S., Macrì, S., Rizzo, A.: Game theoretical trajectory planning enhances social acceptability of robots by humans. Sci. Rep. **12**(1), 21976 (2022)
41. Singh, N.H., Thongam, K.: Neural network-based approaches for mobile robot navigation in static and moving obstacles environments. Intel. Serv. Robot. **12**(1), 55–67 (2019)
42. Xie, Z., Xin, P., Dames, P.: Towards safe navigation through crowded dynamic environments. In: 2021 IEEE/RSJ International Conference on Intelligent Robots and Systems (IROS), pp. 4934–4940. IEEE (2021)
43. Chen, Y. F. , Liu, M., Everett, M., How, J. P.: Decentralized non-communicating multiagent collision avoidance with deep rein-

forcement learning. In: 2017 IEEE international conference on robotics and automation (ICRA), pp. 285–292. IEEE (2017)
44. Chen, C., Liu, Y., Kreiss, S., Alahi, A.: Crowd-robot interaction: crowd-aware robot navigation with attention-based deep reinforcement learning. In: 2019 international conference on robotics and automation (ICRA), pp. 6015–6022. IEEE (2019)
45. Yildirim, Y., Ugur, E.: Learning social navigation from demonstrations with deep neural networks. arXiv preprint (2024)
46. Ramírez, O. A. I. , Khambhaita, H., Chatila, R., Chetouani, M., Alami, R.: Robots learning how and where to approach people. In: 2016 25th IEEE international symposium on robot and human interactive communication (RO-MAN), pp. 347–353. IEEE (2016)
47. Sun, S., Zhao, X., Li, Q., Tan, M.: Inverse reinforcement learning-based time-dependent a* planner for human-aware robot navigation with local vision. Adv. Robot. **34**(13), 888–901 (2020)
48. Johora, F. T., Müller, J. P.: Modeling interactions of multimodal road users in shared spaces. In: 2018 21st International Conference on Intelligent Transportation Systems (ITSC), pp. 3568–3574. IEEE (2018)
49. Hoogendoorn, S., Bovy, P.H.L.: Simulation of pedestrian flows by optimal control and differential games. Optim. Control Appl. Methods **24**(3), 153–172 (2003)
50. Rahmati, Y., Talebpour, A.: Learning-based game theoretical framework for modeling pedestrian motion. Phys. Rev. E **98**(3), 032312 (2018)
51. Rudenko, A., Kucner, T.P., Swaminathan, C.S., Chadalavada, R.T., Arras, K.O., Lilienthal, A.J.: Thör: human-robot navigation data collection and accurate motion trajectories dataset. IEEE Robot. Autom. Lett. **5**(2), 676–682 (2020)
52. Zanlungo, F., Ikeda, T., Kanda, T.: Social force model with explicit collision prediction. Europhys. Lett. **93**(6), 68005 (2011)
53. Ferrer, G., Garrell, A., Sanfeliu, A.: Robot companion: a social-force based approach with human awareness-navigation in crowded environments. In: 2013 IEEE/RSJ international conference on intelligent robots and systems, pp. 1688–1694. IEEE (2013)
54. Farina, F., Fontanelli, D., Garulli, A., Giannitrapani, A., Prattichizzo, D.: Walking ahead: the headed social force model. PLoS ONE **12**(1), e0169734 (2017)
55. Rios-Martinez, J., Spalanzani, A., Laugier, C.: From proxemics theory to socially-aware navigation: a survey. Int. J. Soc. Robot. **7**(2), 137–153 (2015)
56. Hall, E.T.: The hidden dimension, vol. 609. Doubleday, Garden City, NY (1966)
57. McNeill, Alexander R.: Energetics and optimization of human walking and running: the 2000 Raymond pearl memorial lecture. Am. J Hum. Biol. **14**(5), 641–648 (2002)
58. Sagratella, S.: Algorithms for generalized potential games with mixed-integer variables. Comput. Optim. Appl. **68**(3), 689–717 (2017)
59. Menon, P.P., Kim, J., Bates, D.G., Postlethwaite, I.: Clearance of nonlinear flight control laws using hybrid evolutionary optimization. IEEE Trans. Evol. Comput. **10**(6), 689–699 (2006)
60. Moreno, L., Garrido, S., Blanco, D., Munoz, M.L.: Differential evolution solution to the slam problem. Robot. Auton. Syst. **57**(4), 441–450 (2009)
61. Aydin, S., Temeltas, H.: Fuzzy-differential evolution algorithm for planning time-optimal trajectories of a unicycle mobile robot on a predefined path. Adv. Robot. **18**(7), 725–748 (2004)
62. Johansson, A., Helbing, D., Shukla, P.K.: Specification of the social force pedestrian model by evolutionary adjustment to video tracking data. Adv. Complex Syst. **10**(supp02), 271–288 (2007)
63. Tensorflow. https://www.tensorflow.org/~overview?hl=it. Accessed on 23 Aug 2023
64. Spatola, N., Kühnlenz, B., Cheng, G.: Perception and evaluation in human-robot interaction: the human-robot interaction evaluation scale (hries)—a multicomponent approach of anthropomorphism. Int. J. Soc. Robot. **13**(7), 1517–1539 (2021)
65. Truong, X.-T., Ngo, T.D.: Toward socially aware robot navigation in dynamic and crowded environments: a proactive social motion model. IEEE Trans. Autom. Sci. Eng. **14**(4), 1743–1760 (2017)
66. Biswas, A., Wang, A., Silvera, G., Steinfeld, A., Admoni, H.: Socnavbench: a grounded simulation testing framework for evaluating social navigation. ACM Transactions on Human-Robot Interaction (THRI) **11**(3), 1–24 (2022)
67. Gao, Y., Huang, C.-M.: Evaluation of socially-aware robot navigation. Front. Robot. AI **8**, 721317 (2022)
68. Neggers, M. M. , Cuijpers, R. H. , Ruijten, P. A., IJsselsteijn, W. A.: The effect of robot speed on comfortable passing distances. Front. Robot. AI 9:915972 (2022)
69. Prajapati, B., Dunne, M., Armstrong, R.: Sample size estimation and statistical power analyses. Optom. Today **16**(7), 10–18 (2010)
70. Erdfelder, E., Faul, F., Buchner, A.: Gpower: a general power analysis program. Behav. Res. Methods. Instrum. Comput. **28**(1), 1–11 (1996)
71. Chin, R., Lee, B. Y.: Principles and practice of clinical trial medicine. Elsevier (2008)
72. Jolliffe, I.T., Cadima, J.: Principal component analysis: a review and recent developments. Philos. Trans. A Math. Phys. Eng. Sci. **374**(2065), 20150202 (2016)
73. Preferred walking speed. https://en.wikipedia.org/~wiki/~Preferred_walking_speed. Accessed: 2023
74. Joosse, M., Sardar, A., Lohse, M., Evers, V.: Behave-ii: the revised set of measures to assess users' attitudinal and behavioral responses to a social robot. Int. J. Soc. Robot. **5**, 379–388 (2013)
75. Carpinella, C. M., Wyman, A. B., Perez, M. A., Stroessner, S. J., The robotic social attributes scale (rosas) development and validation. In: Proceedings of the 2017 ACM/IEEE International Conference on human-robot interaction, pp. 254–262. (2017)
76. De Graaf, M.M., Allouch, S.B.: Exploring influencing variables for the acceptance of social robots. Robot. Auton. Syst. **61**(12), 1476–1486 (2013)
77. Castro-González, Á., Admoni, H., Scassellati, B.: Effects of form and motion on judgments of social robots' animacy, likability, trustworthiness and unpleasantness. Int. J. Hum Comput Stud. **90**, 27–38 (2016)
78. Average human height by country. https://en.wikipedia.org/~wiki/~Average_human_height_by_country. Accessed: 2023
79. Crowell, C.R., Deska, J.C., Villano, M., Zenk, J., Roddy, J.T.: Anthropomorphism of robots: study of appearance and agency. JMIR Hum. Factors **6**(2), e12629 (2019)

Publisher's Note Springer Nature remains neutral with regard to jurisdictional claims in published maps and institutional affiliations.

Giada Galati received her Ph.D. in Electrical, Electronics and Communications Engineering at Politecnico di Torino in 2024, where she also completed her M.Sc. in Mechatronics Engineering in 2019. Her primary research is in cooperative robotics, focusing specifically on the social acceptability of robots to humans. Her interests also include human-robot interaction in multi-robot systems, with applications spanning unmanned aerial vehicles and autonomous ground vehicles.

Andrea Usai is a Ph.D. student in the Department of Electronics and Telecommunications, Politecnico di Torino, Italy. He received his B.Sc. degree in Mechanical Engineering and the M.Sc. degree in Mechatronics Engineering from the same institution, in 2021 and 2023, respectively. His field of research include robotics, neuro-inspired control architectures, and machine learning, with a focus on nonlinear systems and applications to UAVs and mobile robots.

Giacomo Vignolo works as a System Test Engineer in the aerospace industry with a background in mechatronics and control engineering. He received his Bachelor's degree in Mechanical Engineering in 2021 and his Master's degree in Mechatronics Engineering in 2023 from Politecnico di Torino, where he carried out his Master's thesis at the Department of Electronics and Telecommunications. His research interests focus on robotics and system modeling, with applications to advanced engineering systems.

Simone Macrì Senior Scientist at the Italian National Institute of Health - obtained his PhD in Neuroscience and Natural Sciences at the Swiss Federal Institute of Technology Zurich in 2005. He has been a research fellow at McLean Hospital in Boston and at New York University. Author of over 100 articles in international scientific journals, he coordinates projects funded by the European Community, the Italian Space Agency, the National Research Council, and the Italian Ministry of Health. His research interests span from the biological determinants of mental disorders to the study of social behavior. He has also published popular science books aimed at the general public and younger readers.

Alessandro Rizzo is an Associate Professor at the Department of Electronics and Telecommunications, Politecnico di Torino, Italy, where he coordinates the Complex Systems Laboratory. He received his Laurea degree in Computer Engineering, summa cum laude, and his PhD in Automation and Electronics Engineering from the University of Catania, in 1996 and 2000, respectively. Dr. Rizzo's previous affiliations include JET Joint Undertaking, ST Microelectronics, the University of Messina, Politecnico di Bari, and New York University. His research interests span complex networks and systems, robotics, and the modeling and control of nonlinear systems. He has authored one book, holds two international patents, and has published over 200 papers in peer reviewed international journals and conference proceedings. A Distinguished Lecturer for the IEEE Nuclear and Plasma Sciences Society, he received the Best Application Paper Award at the 2002 IFAC World Congress, as well as two Amazon Research Awards in Robotics (2019,2021).